[Frontiers in Bioscience S2, 939-968, June 1, 2010]

# Physiological modeling for technical, clinical and research applications

**Dusan Fiala[1,2], Agnes Psikuta[3], Gerd Jendritzky[4], Stefan Paulke[5], David A. Nelson[6], Wouter D. van Marken Lichtenbelt[7], Arjan J.H. Frijns[8]**

*[1]ErgonSim – Comfort Energy Efficiency, Holderbuschweg 47, D-7056 Stuttgart, Germany, [2]IBBTE, University of Stuttgart, Keplerstr. 11, 70174 Stuttgart, Germany,[3]Empa, Swiss Federal Laboratories for Materials Testing & Research, Laboratory for Protection and Physiology, Lerchenfeldstrasse 5, CH-9014 St. Gallen, Switzerland, [4]Meteorological Institute, University of Freiburg, Werthmannstr. 10, D-79085 Freiburg, Germany, [5]P+Z Engineering GmbH, Anton-Ditt-Bogen 3, D-80939 Munich, Germany, [6]Department of Mechanical Engineering, University of South Alabama, EGCB 212, 307 University Blvd N. Mobile, AL 36688-0002, USA, [7]Department of Human Biology, Maastricht University, P.O. Box 616, 6200 MD Maastricht, The Netherlands, [8]Department of Energy Technology, Eindhoven University of Technology, P.O. Box 513, 5600 MB Eindhoven, The Netherlands*

## TABLE OF CONTENTS



## 1. ABSTRACT

Various and disparate technical disciplines have identified a growing need for tools to predict human thermal and thermoregulatory responses to environmental heating and cooling and other thermal challenges such as anesthesia and non-ionizing radiation. In this contribution, a dynamic simulation model is presented and used to predict human thermophysiological and perceptual responses for different applications and situations. The multi-segmental, multi-layered mathematical model predicts body temperatures, thermoregulatory responses, and components of the environmental heat exchange in cold, moderate, as well as hot stress conditions. The incorporated comfort model uses physiological states of the human body to predict thermal sensation responses to steady state and transient conditions. Different validation studies involving climate-chamber physiological and thermal comfort experiments, exposures to uncontrolled outdoor weather conditions, extreme climatic and radiation asymmetry scenarios revealed the model to predict physiological and perceptual responses typically within the standard deviation of the experimental observations. Applications of the model in biometeorology, clothing research, the car industry, clinical and safety applications are presented and discussed.

## 2. INTRODUCTION

Fast technological developments and the ever-increasing complexity of new technological products require novel, intelligent ergonomic solutions. The "human factor" has become central to many of these endeavors. Over the past ten to fifteen years, there has been a steadily growing demand from research and industry for reliable models simulating human thermal and perceptual responses in various technical applications. The imperative for adequate simulation of human thermoregulatory behaviors, better understanding of related performance and safety limits, and optimum conditions for well-being and comfort has never been greater.

Mathematical modeling of the human thermal system goes back 70 years starting with general heat balance considerations (1, 2, 3) followed by various two-node models of human thermoregulation, and human heat budget thermal comfort models (4, 5, 6, 7). Besides numerical modeling, empirical-research approaches emerged. The adaptive comfort model which is based on observations from field studies from around the world gained significance mainly in the building sector (8, 9). In the past forty years, simple two-node (core and skin) models have evolved to more sophisticated, multi-segmental models (10, 11, 12, 13). The latter simulate human heat transfer phenomena inside the body and at its surface taking into account anatomical, thermal and physiological properties of the human body and the thermoregulatory responses of the central nervous system. Besides overall thermophysiological reactions, they also predict "local" characteristics such as skin temperatures and sweat rates of individual body parts.

Mathematical models have been valuable tools (e.g. 10, 11) contributing to a deeper understanding of the principles of human thermoregulation. Nevertheless models have not gained widespread use. The reasons might include: lack of confidence in their predictive abilities; limited range of applicability; and/or poor modeling of the heat exchange with the environment. Usually (e.g. 10), models have been *postulated* based on a limited number of experiments and test-subjects and often, authors have used their own experiments rather than independent experimental data to validate models. Comprehensive validation studies against independent experimental data have not or been seldom carried out.

One of the new-generation, multi-node models of human thermoregulation and thermal comfort is the Fiala human Physiology and thermal Comfort (FPC) model. The FPC-model is a numerical framework of models which – linked together – predict human thermophysiological and thermal sensation responses to wide ranging steady and transient boundary conditions. The stimulus for the work was the desire to make available products of fundamental physiological research to scientists, engineers and designers working in other disciplines. These include architecture, automotive and aerospace industries, biometeorology, textile and clothing research, research into health and safety in extreme conditions, and medical engineering.

The fundamental modeling work was conducted at the University of Applied Sciences Stuttgart in Germany – in collaboration with the De Montfort University (DMU), UK (14). This work was followed by applied research and diverse applications of the model at the Institute of Energy and Sustainable Development (IESD) at DMU. At IESD the model has been used in a variety of "real world" projects, such as the design of the Sydney 2000 Olympics Stadium (15), buildings equipped with energy-efficient passive downdraft evaporative cooling (PDEC) systems (16), and the development of a simulation system for predicting comfort responses in automobiles (17). These activities furthermore included research into modeling of the human occupancy factor in the design of naturally ventilated buildings (18), and modeling human comfort responses to asymmetric radiation (19).

Research work concerned with the application of the FPC-model and the development of "physiologically intelligent" thermal manikins for clothing research has been carried out at the Swiss Federal Laboratories for Material Testing and Research (Empa) in Sankt Gallen, Switzerland (20). Engineers of P+Z Engineering GmbH, have conducted significant modeling efforts implementing the FPC-model algorithms in a sophisticated multi-model simulation system for detailed comfort analysis in cars (21). Researchers and engineers of the Michigan Technological University, Houghton, MI and ThermoAnalytics Inc., Calumet, MI developed techniques for fast and detailed human radiation exposure analysis and detailed human body models for clinical applications (22, 23). Researchers of Maastricht University and Eindhoven University of Technology, The Netherlands, adapted the FPC-model for individuals (24) and developed a simulation system for predicting physiological responses of anesthetic patients during open-heart surgery (25). Most recently the FPC-model has been used as a basis for developing the Universal Thermal Climate Index (UTCI) of the EU COST Action 730 for assessing the combined effect of outdoor climate condition on humans (26).

This contribution describes the FPC-model and provides an overview of the various applications and advances made in modeling human thermal responses in technical and clinical disciplines.

## 3. FPC-MODEL

From the mathematical point of view the human organism can be considered as two interacting systems of thermoregulation: the controlling *active system* and the controlled *passive system*. While the passive system simulates the physical human body and the heat and mass transfer within the body and at its surface, the active system mimics the behavior of the human temperature regulation system predicting responses of the central nervous system.

### 3.1. Passive system

The passive system of the FPC-model is a multi-segmental, multi-layered representation of the human body. The body is idealized as 20 spherical and cylindrical elements: head, face, neck, thorax, abdomen, hip, left and

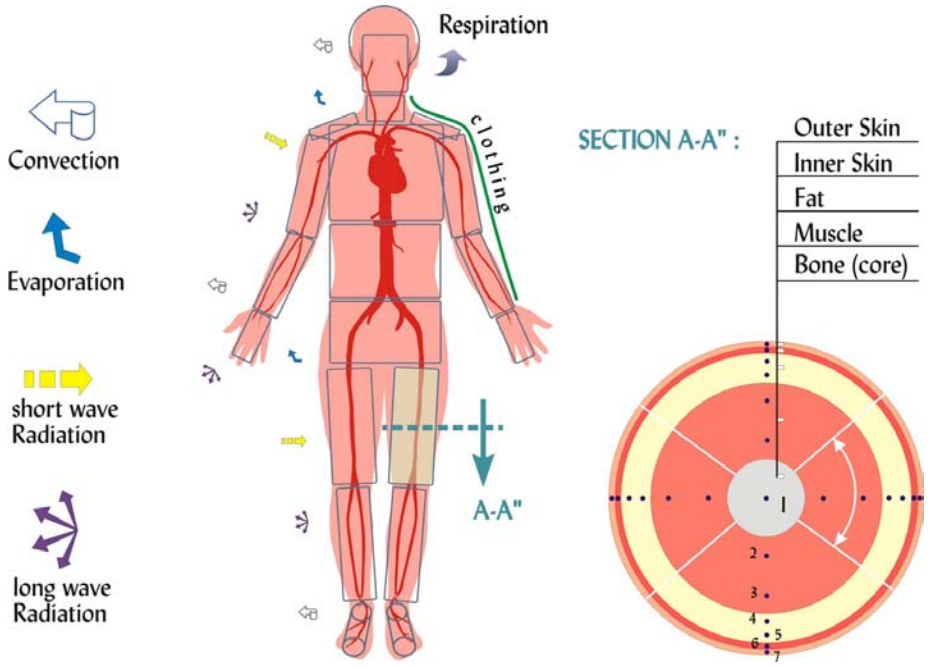


**Figure 1.** Passive system of the FPC-model.

right shoulders, and left and right extremities: upper and lower arms, hands, upper and lower legs, feet (Figure 1). Body elements are subdivided further laterally into sectors (in total 63) to enable simulation of spatial asymmetric boundary conditions.

Each body element is built of annular concentric tissue layers (section A-A″ in Figure 1) of appropriate thermophysical properties and basal physiological functions of different tissue materials: brain, lung, bone, muscle, viscera, fat, and skin (27). In accordance with Weinbaum *et al* (28), skin is modeled as inner and outer cutaneous layer. The inner skin simulates the cutaneous plexus - a blood-perfused region in which also some metabolic heat is produced. The outer skin contains neither heat sources nor thermally significant blood vessels. This superficial skin layer is of importance for modeling skin evaporation: it contains sweat glands and simulates the vapor barrier for moisture diffusion through the skin.

The FPC computer humanoid represents an "average" person with a body weight of 73.4 kg, body fat content of 14%wt, and a Dubois-area of 1.85 m². The physiological data aggregated to a basal whole body heat output of 87.1 W corresponding to 0.8 met for a reclining person, basal evaporation rate from the skin of 18 W, and basal cardiac output and skin blood flow rate of 4.9 L $min^{-1}$ and 0.4 L $min^{-1}$, respectively (27). The basal physiological data is appropriate for an adult in a thermo-neutral environment of 30 °C. In these conditions (where no thermoregulation occurs) the model predicts a basal skin wettedness of 6%; a mean skin temperature of 34.4 °C; and body core temperatures of 37.0 °C in the head core (hypothalamus) and 36.9 °C in the abdomen core (rectum) (27).

Within the human body, metabolic heat is generated, stored, and conducted from warmer to colder tissue regions and is distributed over the body by blood circulation. The mechanisms of the dynamic heat transfer within the living tissue are simulated using the Pennes' *Bio-Heat Transfer Equation* (3) formulated for polar and spherical coordinates in the model:

$$\rho c \frac{dT}{dt} = k\left(\frac{d^2T}{dr^2} + \frac{g}{r}\frac{dT}{dr}\right) + q_m + \rho_{bl}\, w_{bl}\, c_{bl}\, \left(T_{bla} - T\right)$$

where *rho*, *c*, and *k* are the tissue density [kg $m^{-3}$], heat capacitance [J $kg^{-1}$ $K^{-1}$], and conductivity [W $m^{-1}$ $K^{-1}$], respectively. *T* is the tissue temperature [°C], *t* time [s], *r* radius [m]; *g* a geometry factor (equal to 1 and 2 for polar and spherical co-ordinates, respectively), $q_m$ metabolism [W $m^{-3}$], $rho_{bl}$ blood density [kg $m^{-3}$], $w_{bl}$ blood perfusion rate [$m^3$ $s^{-1}$ $m^{-3}$], $c_{bl}$ heat capacitance of blood [J $kg^{-1}$ $K^{-1}$], and $T_{bla}$ [°C] arterial blood temperature.

In the numerical model each tissue layer is discretized as one or more tissue nodes (see Figure 1 section A-A" for nodal spacing in the left upper leg). In the actual version of the FPC-model, this accumulates to a total of 366 tissue nodes for the body as a whole. A numerical form of the *Bio-Heat Transfer Equation* is applied to each node using appropriate basal tissue material properties. In addition to the original Pennes' approach, counter-current heat exchanges between adjacent arteries and veins are considered. The system of coupled equations is solved using appropriate hybrid matrix solution techniques (14).

At the body surface, heat is exchanged by free and forced convection with air, long and short wave

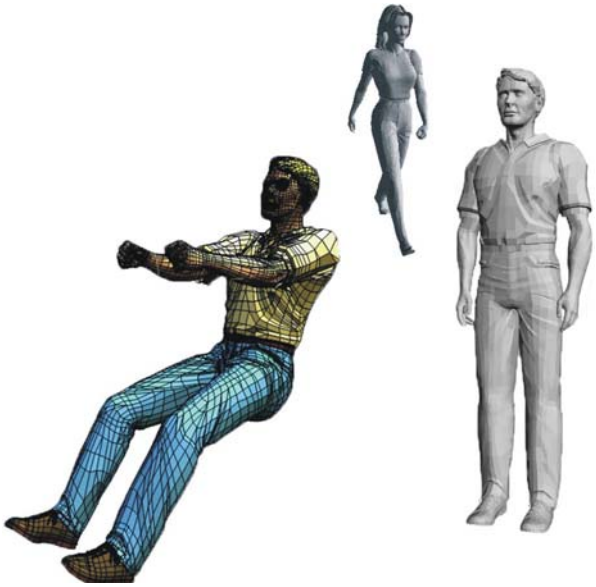

**Figure 2**. 3D human geometry models for detailed human heat transfer analysis.

radiation, and evaporation of moisture from the skin. Part of the bodily heat is lost by respiration. The local surface heat losses vary from one body part to another due to asymmetric environmental conditions, non-uniform clothing and/or local regulatory and temperature responses. The multi-segmental model takes such inhomogeneities into account by establishing local heat and mass balances for each spatial body sector (27). This allows the model to be coupled with other simulation tools predicting, for example, the thermal conditions to which humans are exposed in cars, buildings and other artificial indoor or natural outdoor environments. Over the past years significant research efforts have been undertaken to develop sophisticated coupled (numerical as well as physical) simulation systems for application in different areas of research and technical development (17, 18, 21, 29, 30). Some of the coupled systems developed recently involving the FPC-model are described further below.

Realistic representation of the three-dimensional human body geometry and its local characteristics forms a basis for detailed human heat transfer analysis. Various specialist software tools are now available to facilitate the development of realistic static as well as moving humanoid geometry models, considering differences in male and female anthropometric data and body postures (Figure 2).

Human-environment thermal interactions play an important role in numerous areas of human endeavor. Industrial applications often require detailed simulation of the complex heat and mass transport processes under real-world, non-uniform and transient scenarios to assess their impact on human physiological and perceptual states. Sophisticated specialist software is then needed to aid realistic predictions of the micro-climatic conditions which surround humans and to simulate the thermal processes that occur between the temperature-regulated human body and the immediate environment.

The need for detailed simulations of personal exposure to indoor environments and contaminant movement has been a motivation of a continuously growing number of numerical studies using so-called computer simulated persons (CSP) and computational fluid dynamics (CFD) codes. CFD is capable of solving complex conjugate heat transfer problems predicting spatial variations of air temperature, air velocity, turbulence intensity, air moisture content and pollutant concentrations. While CSPs typically are simplified representations of the sole human body geometry, coupled simulation systems recently have been developed to synergize the predictive capabilities of CFD and FPC models (30, 18, 31). These systems advance our ability to simulate human-environment thermal interactions, the micro-climatic conditions surrounding humans (Figure 3) aimed to facilitate the design of comfortable, energy efficient buildings.

Radiative heat exchange with the environment and high intensity sources has important implications for human health and safety (32), well-being and comfort (33). In buildings, occupants are often exposed to inhomogeneous radiation, for example, in the proximity of cold windows, hot radiators, or due to solar radiation transmitted through glazed façades. In cars and aircraft cabins such uncomfortable conditions slow down the reactions of drivers and pilots. Critical, life-threatening situations can arise for fire-fighters or factory workers exposed to IR-radiation from fire or other high intensity sources.

Today's state-of-the-art radiation analysis tools include advanced numerical techniques, such as the voxel-based ray tracing method (22), to enable fast and accurate radiation simulations even for highly complex geometries. A voxel may be thought of as a three-dimensional analog of a pixel. Linked with physiological predictions fast and

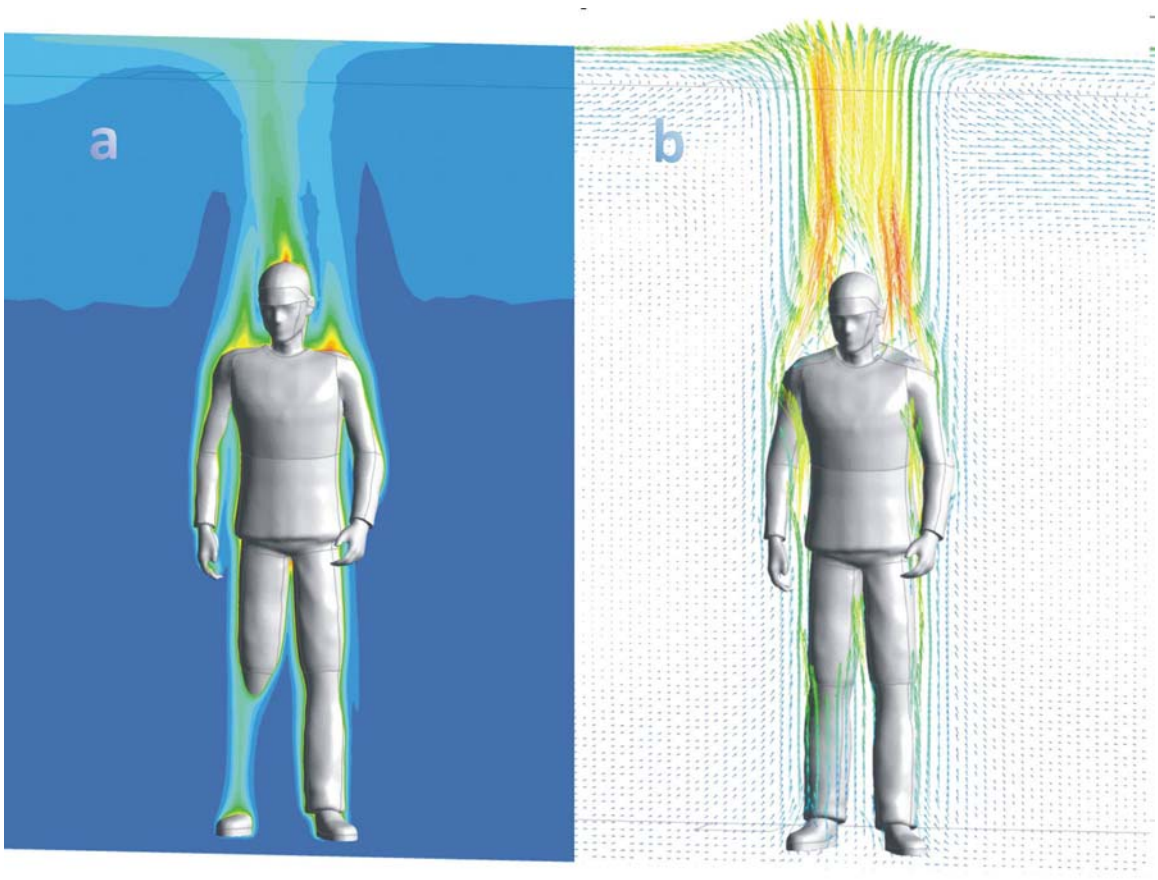


**Figure 3**. Temperature (a) and air velocity (b) distribution around a temperature-regulated human body predicted by coupled CFD-FPC-model simulation (18).

detailed computer-aided analysis of the dynamic long-wave and short-wave radiation effects on humans (34, 35) has so become possible (Figure 4). Physiological comfort models for predicting human local or global perceptual responses to asymmetric radiation scenarios involving the FPC-model have been developed and used (17, 19, 31) to assess, for instance, the comfort conditions in cars (17) the implications of seasonal comfort in the perimeter zones of buildings (19) or to quantify the comfort performance of window systems as a method for defining new, human-factor-related, classification criteria of such technical products (36).

### 3.2. Active system

The active system of the FPC-model predicts the four essential overall thermoregulatory responses of the central nervous system, their regional distributions and modulations due to local thermal influences: shivering (SH), sweating (SW), and peripheral vasomotion, i.e., dilatation (DL) and constriction (CS). This cybernetic model was developed based on simulation and statistical regression analysis of independent experimental studies provoking the above responses of unacclimatized subjects under different scenarios (37). The experiments were selected through a literature survey covering a range of environmental temperatures from 5ºC to 50ºC and exercise intensities between 0.8 met and 10 met.

Measured regulatory responses were correlated with predicted afferent signals associated with the mean skin temperature, $T_{sk,m}$, the head core temperature, $T_{hy}$, as well as theoretically possible signals such as the mean muscle temperature, $T_{msc,m}$, and the mean skin heat flux, $Q_{sk,m}$ (Figure 5). Regression analysis was employed to investigate (i) the involvement and responsibility, i.e., statistical significance, of individual afferent signals and (ii) to formulate the governing control equations for individual responses (37).

The regression analysis studies confirmed $T_{hy}$ and $T_{sk,m}$ to be the main driving impulses for regulatory actions (37). An additional signal, i.e., the rate of change of the mean skin temperature, $dT_{sk,m}/dt$, weighted by the error signal of the skin temperature, ($T_{sk,m}$-34.4), was identified as the driving impulse for dynamic events in thermoregulatory reactions to cold such as the shivering ”overshoot” (Figure 6). This effect is typically observed in subjects suddenly exposed to cold environmental conditions. In the experiment (38) the test-subjects underwent a step change in air temperatures from 24 to 5

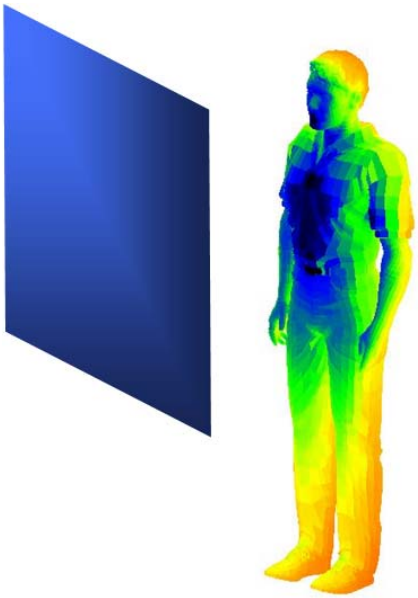

**Figure 4**. Local body cooling / surface temperature distribution of a person exposed to long-wave radiation heat exchange with a cold window.

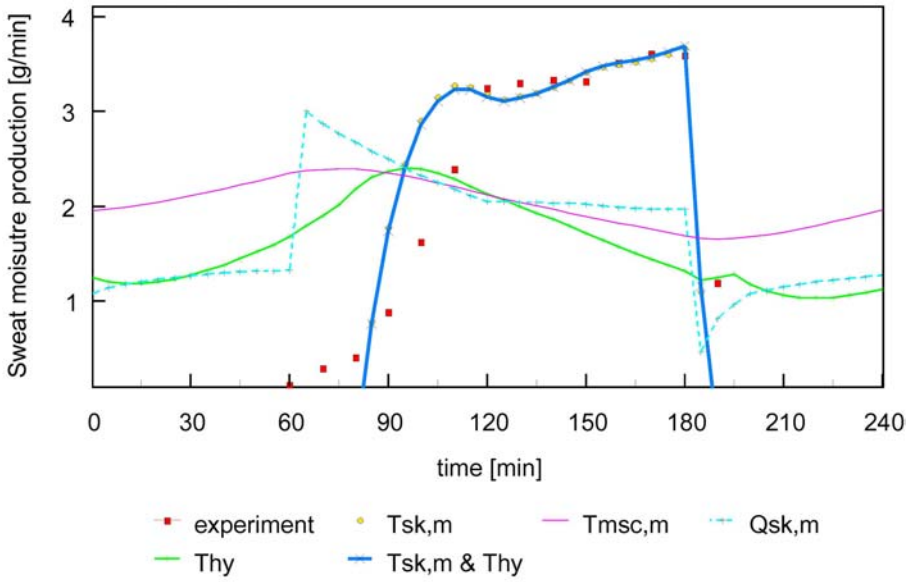


**Figure 5**. Regression lines obtained for sweating in response to sudden changes in air temperature from 18 °C to 42 °C (time>60 min) and back again (time>180 min).

°C where they stayed reclining for 90 minutes. Under those conditions the signal associated with $T_{sk,m}$ was the best single ”static” predictor of SH for t>40 min. The overshoot at t=10 min, however, could not be explained by $T_{sk,m}$. Rather, the product $(T_{sk,m} - 34.4)\cdot dT_{sk,m}/dt$ reproduced the nature of this event, indicating the existence of an additional, specifically dynamic component in the thermoregulatory response of shivering.

The linear regression analyses were carried out for each experiment studied. The results were then subjected to a further, supra-experimental, analysis to study the consistency of the results obtained for individual exposures and to investigate any potential functional dependencies of the regression coefficients on thermal states of the subjects associated with an exposure (37). Interestingly, the supra-experimental analysis revealed that, for example, although sweating can be described sufficiently by skin- and head core temperatures over the whole range of the conditions considered, the relative contributions of the individual signals are not constant. In resting subjects exposed to warm and hot environments, sweating was dominated by elevated skin temperature as a punitive signal. This was associated with regression

**Table 1.** Active system control coefficients

| | SH | CS | DL | SW |
|---|---|---|---|---|
| Coeff. | [W] | [ - ] | [W/K] | [g/min] |
| $A_1$ | 10.00 | 35.00 | 21.00 | 0.80 |
| $A_2$ | 0.48 | 0.34 | 0.79 | 0.59 |
| $A_3$ | 3.62 | 1.07 | -0.70 | -0.19 |
| $A_4$ | -10.00 | -35.00 | 21.00 | 1.20 |
| $B_1$ | 0.00 | 0.00 | 32.00 | 5.70 |
| $B_2$ | 0.00 | 0.00 | 3.29 | 1.98 |
| $B_3$ | 0.00 | 0.00 | -1.46 | -1.03 |
| $B_4$ | -27.90 | 0.00 | 32.00 | 6.30 |
| C | 1.70 | 3.90 | 0.00 | 0.00 |
| D | -28.60 | 0.00 | 0.00 | 0.00 |

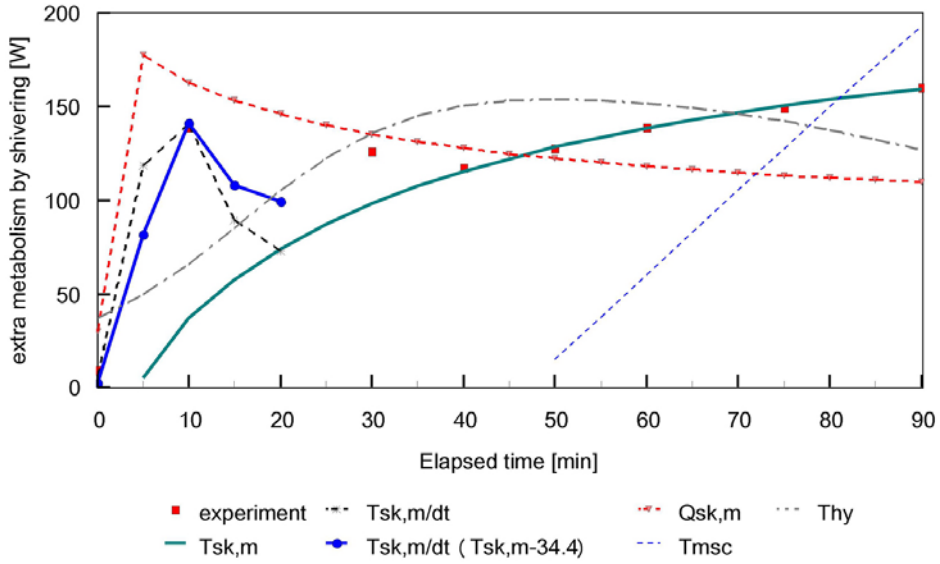


**Figure 6**. Linear regression lines for the shivering response following a sudden exposure to cold air of 5 °C.

coefficients $b_{sw,sk}$, that were higher than coefficients obtained for subjects sweating in the cold (Figure 7a). In exercising subjects exposed to cold or moderate conditions, on the other hand, the impact of body core temperature on sweating rose with elevating internal heat strain, which was associated with rising values of regression coefficients, $b_{sw,sk}$ (Figure 7b).

As a result, the following non-linear relationship was developed (with coefficients listed in Table 1) governing individual thermoregulatory responses, F, for wide-ranging boundary conditions:

$$F = \left\langle A_1 \, tanh\left[A_2 (T_{sk,m} - 34.4) + A_3\right] + A_4 \right\rangle (T_{sk,m} - 34.4) +$$
$$\left\langle B_1 \, tanh\left[B_2 (T_{hy} - 37.0) + B_3\right] + B_4 \right\rangle (T_{hy} - 37.0) +$$
$$+ C \, \Delta T_{sk,m} \dot{T}_{sk,m} + D$$

A schematic diagram of the FPC active system is presented in Figure 8. The central nervous system thermoregulation accounts for overall changes in muscle metabolism via shivering (and the corresponding changes in muscle blood flow), changes in skin blood flow via vasodilatation and vasoconstriction, and for sweating as autonomic regulatory responses. Included is also the sensation of thermal comfort as a response for behavioral thermoregulation. The local autonomic regulation utilizes local skin and tissue temperatures, $T_{sk,i}$ and $T_i$, to modulating local sweat rates, blood flows, and tissue metabolic rates.

### 3.3. Thermal sensation

Current international standard thermal comfort models (39, 40) predict human thermal sensation levels on the basis of an overall heat balance of the body for combinations of environmental and personal parameters for moderate, *steady-state* conditions (7). The physiological principles of human temperature sensation and comfort, particularly in transients and during exercise, are however less well understood.

The FPC thermal comfort model was developed based on simulation and regression analysis of available comfort experiments covering different static and transient environmental temperatures, relative humidities, and exercise intensities (41). Altogether, 220 exposures involving over 2000 male and female test subjects covering a range of air temperatures between $13<T_a<48$ °C and activity levels between 1 and 10 met were simulated and analyzed.

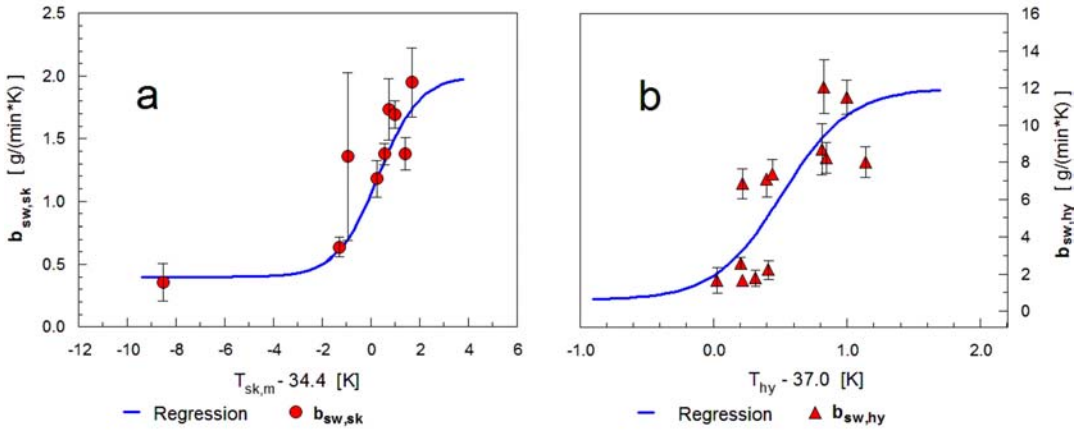


**Figure 7**. Regression coefficients obtained for the sweating response in different exposures (37).

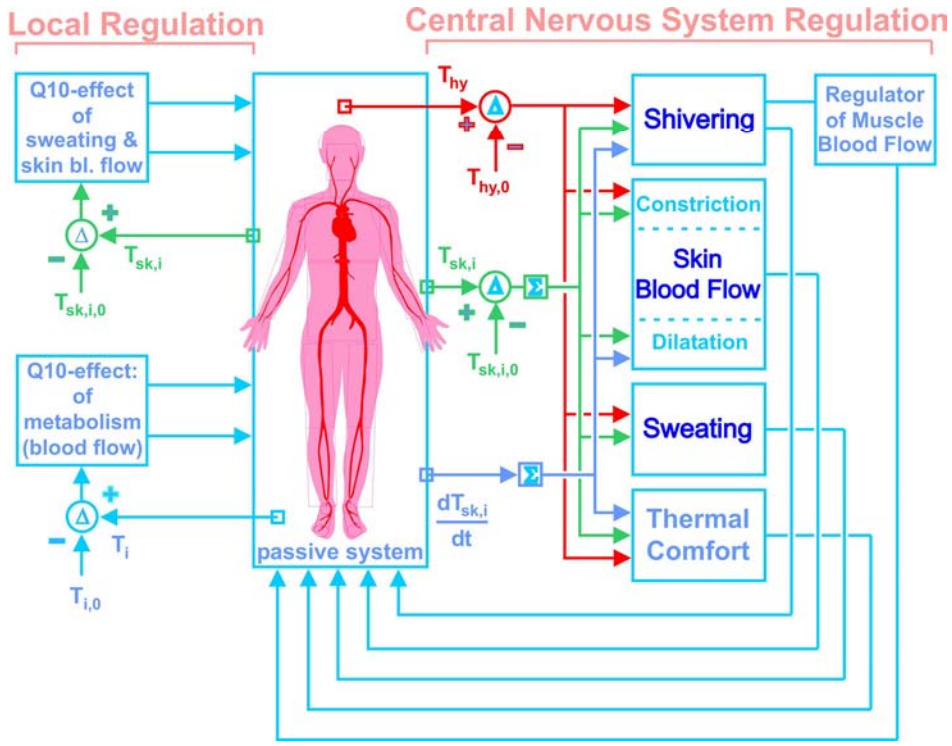


**Figure 8**. Schematic diagram of the FPC active system. feedback system with local skin and tissue temperatures, head core (hypothalamus) temperature and the rate of change of skin temperature as input signals. The setpoint temperatures $T_{sk,i,0}$, $T_{i,0}$ and $T_{hy,0}$ refer to the body's thermo-neutral state at 30 °C room temperature (described above).

Regression analysis of measured sensation votes and simulated data revealed temperature signals from the skin and the head core, and the rate of change of the skin temperature to be the driving impulses which govern the human overall Thermal Sensation, TS. Here, TS (which is not identical with the subjective sensation of thermal comfort) is defined according to the 7-point ASHRAE thermal sensation scale (39) running from -3 (cold) over 0 (neutral) to +3 (hot). Skin temperature was found to be the best predictor of TS across the whole spectrum of the analyzed (steady-state) environmental conditions for sedentary subjects. In cool/cold and even in warm environments, TS correlated better with skin temperature than with other physiological variables, such as internal temperature, sweat rate, or changes in skin blood flow (Figure 9).

Body core temperature was identified as a further important afferent signal in exercising subjects affecting TS in complex, non-linear fashion. The contribution, G, of the

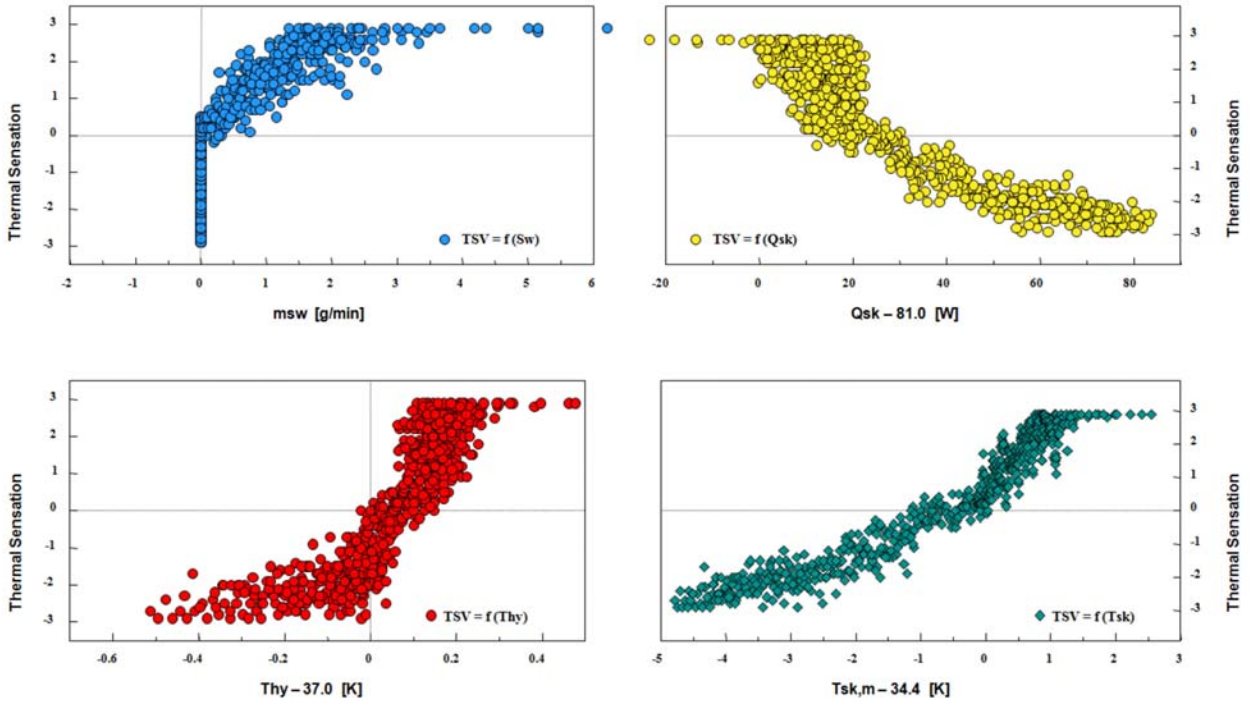


**Figure 9**. Correlation of thermal sensation votes observed in sedentary subjects for air temperatures and relative humidities between 15.6<$T_a$<36.7 °C and 15<RH<85 %, respectively, with predicted sweat rates, $m_{sw}$, and "error signal" values of the overall skin heat flux, head core temperature, and mean skin temperature.

core temperature is a composite of influences from both the body core, $g_{hy}$, and the skin, $g_{sk}$ (Figure 10): $G = g_{hy} \cdot g_{sk}$ (41).

Furthermore, regression analysis of perceptual responses to fast-changing environmental conditions indicated a strong dynamic component in the human sensation of temperature. Both negative and positive rates of change of the mean skin temperature, $dT_{sk,m}/dt$, were identified as the physiological origin of such transient effects. The dynamic thermal sensation, DTS, which includes both static and dynamic input signals is described as (41):

$$DTS = 3 \times \tanh\left(\frac{0.11\frac{dT^{-}_{sk,m}}{dt} + 1.91\frac{dT^{+}_{sk,m}}{dt_{\max}}e^{-0.681t}}{1+G} + \right.$$
$$\left. + m\,(T_{sk,m} - 34.4) + G\right)$$

where $m$ is 0.30 $K^{-1}$ and 1.08 $K^{-1}$ for $T_{sk,m}$<34.4 °C and $T_{sk,m}$>34.4 °C, respectively; $dT^{-}_{sk,m}/dt = 0$ for $dT_{sk,m}/dt > 0$, $dT^{+}_{sk,m}/dt_{max}$ the maximum positive rate of change of skin temperature, $t$ the time elapsed since the occurrence of $dT^{+}_{sk,m}/dt_{max,}$ and $G$ is calculated by:

$$G = 7.94 \times \exp\left(\frac{-0.902}{T_{hy} - 36.6} + \frac{7.612}{T_{sk,m} - 38.4}\right)$$

### 3.4. Model validation

The FPC-model has been subject to various general (37) as well as application-specific validation studies including indoor climate conditions in buildings (41), transient conditions in cars (17), various asymmetric radiation scenarios (19, 42). A large-scale validation study of the FPC-model was conducted as part of the COST Action 730 project in which the model was validated against measured data from climate chamber/wind tunnel experiments as well as field surveys of exposures to outdoor weather conditions (discussed further below).

The behavior of the model over a range of steady air temperatures between 5 °C and 48 °C (after 1 hr of exposure, semi-nude sedentary subjects) is indicated in Figure 11 where predicted body temperatures and regulatory reactions are compared with measured data from different climate chamber experiments (37). The experimental results are provided as averages with the corresponding standard deviations (SD).

The validation tests included transient exposures to fast-changing environmental conditions such as sudden changes in air temperature, $T_a$. Comparison of predicted temperature and regulatory responses with experimental data measured for step changes from neutral to cold and from hot to cold and back again are shown in Figure 12 and Figure 13, respectively (37).

The inclusion of detailed radiation modeling enables predictions of human physiological responses to

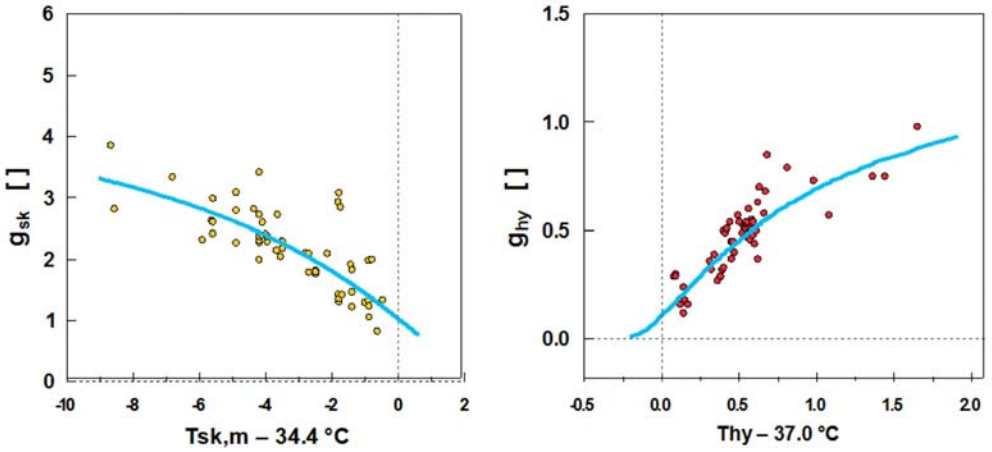


**Figure 10**. The function $g_{sk}$ of the mean skin temperature and $g_{hy}$ of the head core (hypothalamus) temperature.

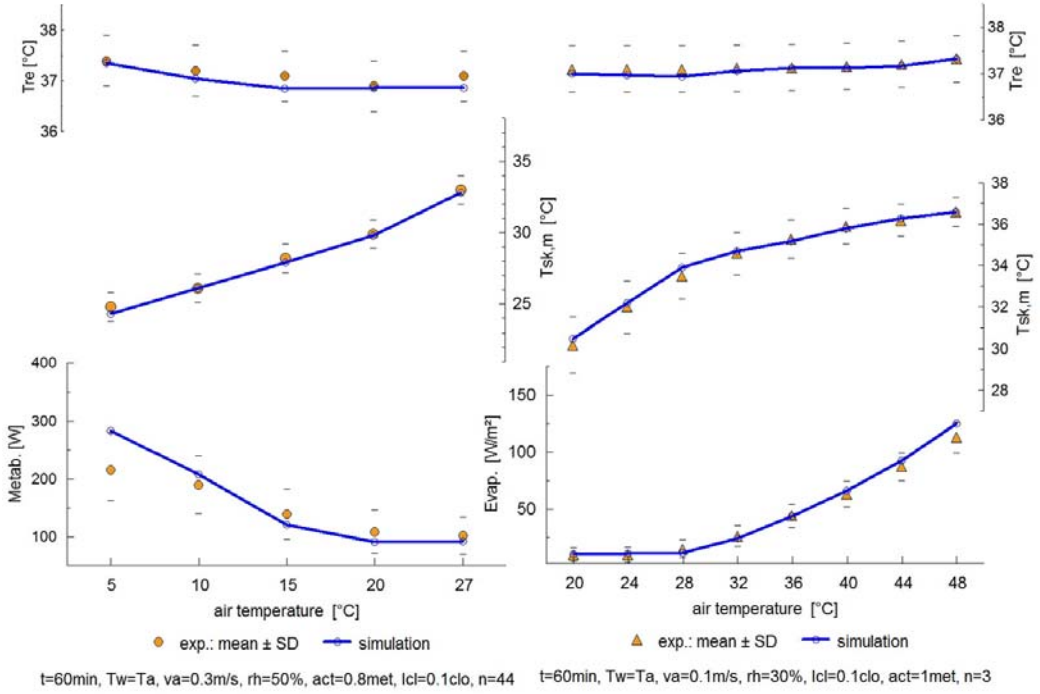


**Figure 11**. Mean skin temperature, body core temperature and thermoregulatory responses as measured and predicted over wide-ranging steady state environmental conditions.

asymmetric environments featuring non-uniform surface temperatures and IR-sources (35, 42). A comparison of predicted and measured skin temperatures for clothed subjects exposed to a range of plane radiant temperature asymmetries between -15 K and +35 K due to chilled and heated walls and ceilings (19) is shown in Figure 14.

The asymmetric radiation exposure tests also included extreme conditions such as those investigated by Hall and Klemm (43). In their experiments the (semi-nude) subjects lay supine on a net in the centre of a chamber which was divided into an upper and lower section. The surfaces of the upper section were maintained at 65, 82, or 93 °C while the lower section surface temperature was at -6.7 or -11°C. This resulted in plane radiant temperature asymmetries of up to 100 K. The average air temperature in the proximity of the subjects was 20 °C, and the average air velocity and water vapor pressure in the chamber were 0.08 m/s and 2.5 mmHg, respectively. The results are plotted in Figure 15. The skin temperatures of individual spatial body sectors were predicted and averaged over the anterior and posterior body parts and for the whole body according to the experimental protocol.

The dynamic behavior of human thermal sensation, as observed experimentally and as predicted by

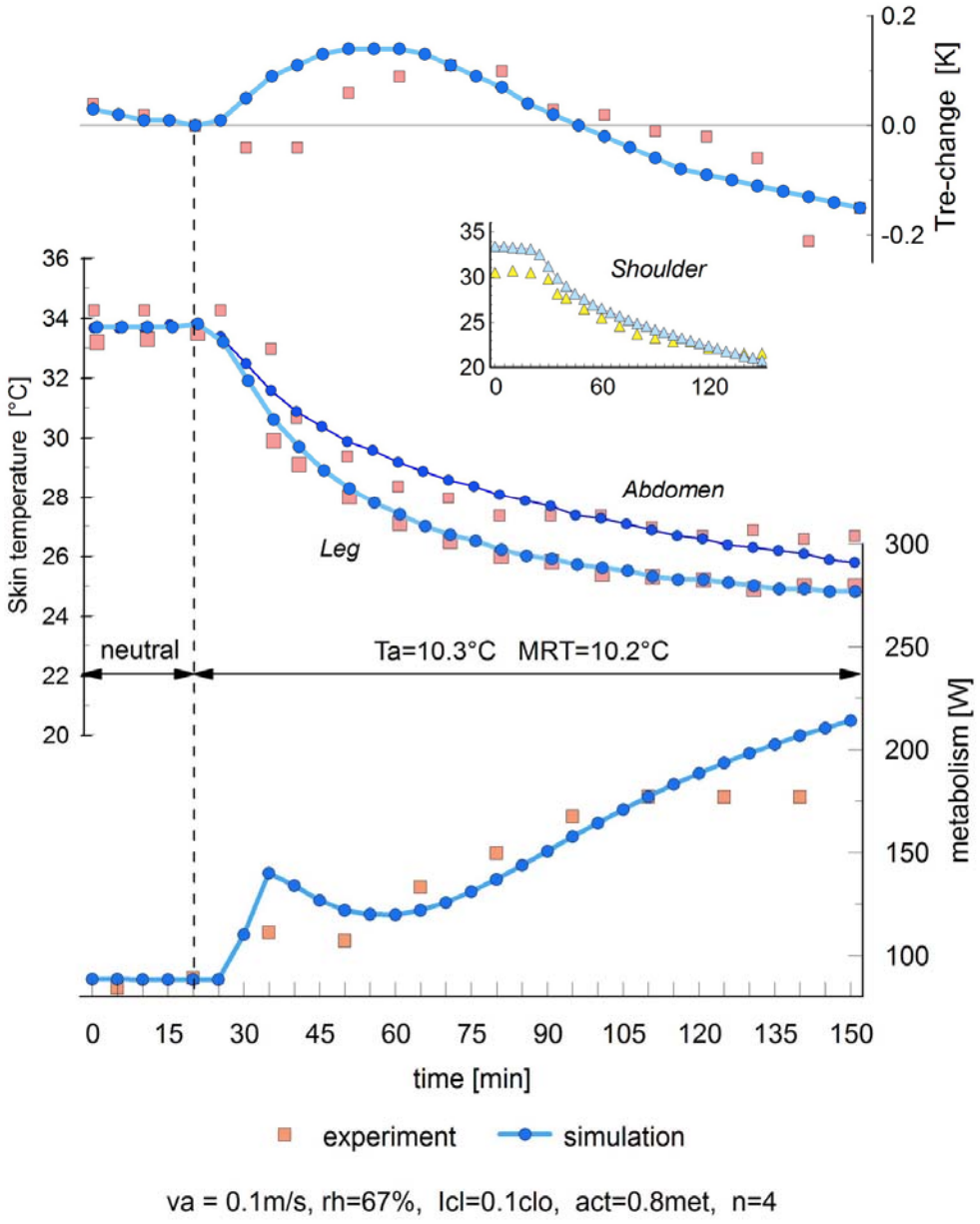


**Figure 12**. Measured and predicted responses of semi-nude, reclining subjects exposed to a cold environment of 10 °C.

the FPC comfort model, is presented for transient environmental conditions, i.e., periodic changes in air temperature, in Figure 16 (41).

In summary, the various validation tests revealed consistent predictions in line with experimental observations for unacclimatized/untrained subjects with respect to thermal regulatory and sensation responses, mean and local skin temperatures and internal temperatures for steady-state and transient boundary conditions, air temperatures ranging between 5 °C and 50 °C and activity levels between 0.8 and 9 met. Mean and local skin temperatures agreed with experimental observations typically within ±1 K, body core temperatures within ±0.5 K, shivering and sweating responses within 50 W, and perceptual responses within ±1 scale units (of the 7-point ASHRAE scale).

## 4. UNIVERSAL THERMAL CLIMATE INDEX

### 4.1. Introduction

In human biometeorology, the combined effect of temperature, wind, humidity and solar radiation is important when assessing the strain caused by outdoor weather on the human organism. Although more than 100 different models and indices exist today (see e.g. ref. 44 for a review), they are either (i) not generally accepted and/or

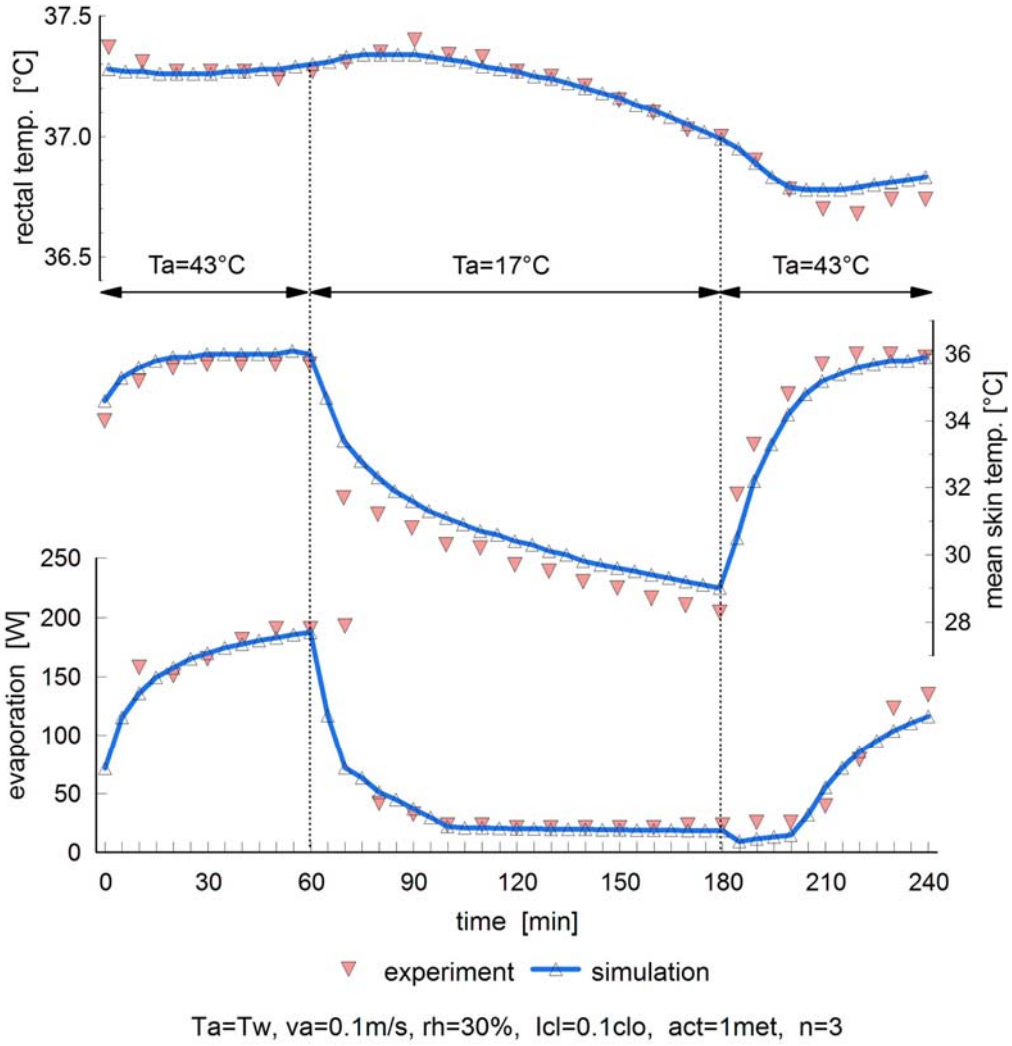


**Figure 13**. Comparison of measured and predicted skin and rectal temperatures and sweating responses for sudden changes in operative temperature.

(ii) restricted to a limited range of environmental conditions.

The International Society of Biometeorology, ISB, recognized the need for a new, widely valid index and established Commission 6 *"On the development of a Universal Thermal Climate Index UTCI"* (45). These efforts have been reinforced in 2005 by launching COST (Cooperation in Science and Technical Development) Action 730 (26). This Action brought together experts in the area of human thermophysiology, physiological modeling, meteorology and climatology from 19 signatory European countries including Israel plus experts from Australia, New Zealand and Canada. The main objective was to develop and make available a physiological response-based assessment index of the thermal environment for applications related to human health and well-being in public weather service, public health system, precautionary planning, and climate impact research.

The proposed new index was to be thermophysiologically significant and valid across the entire spectrum of outdoor weather conditions, including weather extremes. UTCI would consider the complete human heat budget and physiological responses of an average population person. Considering the scientific advances of the past four decades in thermophysiological modeling UTCI should:

- be based on the most advanced multi-node thermophysiological models as reference for obtaining the key results from systematic simulations;
- include the capability to predict both whole body thermal effects (hypothermia and hyperthermia; heat and cold discomfort), as well as local effects (i.e., facial cooling and frostbite);
- represent a temperature-scale index, (i.e., the air temperature of a defined, reference environment);

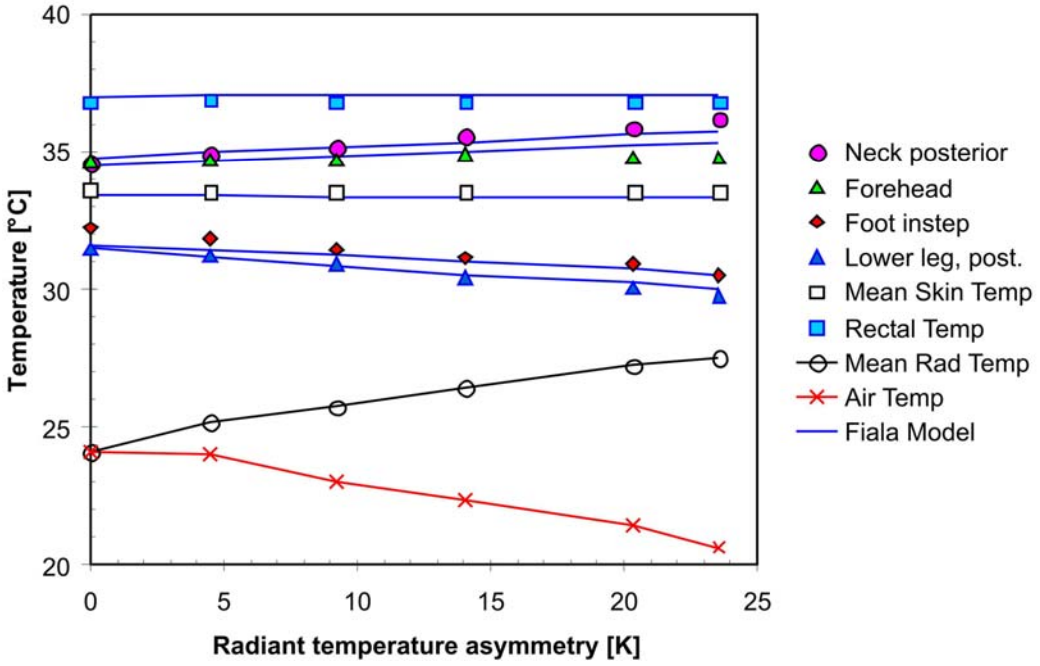


**Figure 14**. Comparison of predicted and measured body and skin temperatures for different levels of radiant asymmetry.

- and be useful for key applications in human biometeorology as noted above.

In order to be easily understood by the general public, UTCI should be a simple index. It is therefore defined as the temperature of a *reference environment* that causes the same physiological strain as the actual environment. The reference environment represents a fictitious, calm air, outdoor climate in which the mean radiant temperature, $T_{MRT}$ (defined to include both short- and long-wave radiation fluxes) is equal to the ambient air temperature. The reference relative humidity is 50% but not exceeding 20hPa partial water vapor pressure.

Based on extensive verification and validation tests and model availability, the COST 730 experts decided to use the FPC multi-node model as an adequate approach for the wide-ranging purposes of the COST Action 730 and to form the basis of the new UTC-Index. For that purpose, a special version of the model (UTCI-Fiala) was created extending the original FPC-model to adequately predict human responses to outdoor weather conditions.

UTCI is a regression model that uses physiological variables predicted by the UTCI-Fiala model including body core and skin temperatures, metabolic, sudomotor and vasomotor regulatory responses as well as the exposure time to characterize the physiological strain of humans exposed to combinations of the prevailing outdoor climate conditions, Figure 17 (46).

**4.2. Model verification and validation**

It was important to ensure that the physiological model to be used to develop UTCI was able to reproduce human thermal and regulatory responses over a broad spectrum of outdoor climate conditions. The model was thus evaluated regarding the plausibility of predicted data; model validity, performance and suitability to predict physiological responses of a (untrained, average, unacclimatized) human. Two approaches were employed to ensure the highest possible validity and applicability of the new UTC-Index: 1. comparison of simulation results obtained using other available multi-node, two-node and simple heat budget models and 2. validation against experimental data involving human subjects.

The model verification work of the COST Action 730 included evaluations of existing human heat budget models regarding their performance and suitability to predict human physiological responses to wide-ranging outdoor climate conditions. This exercise involved comparisons of predicted body and skin temperatures, calorimetric and thermoregulatory responses and plausibility analysis of predicted data based on expert knowledge and expertise. Several published models have been analyzed for their suitability for UTCI-purposes.

The FPC-model was compared with a variety of models, including the new Wind Chill Index (WCI) model (47) in official use in Canada and the US since 2002. To enable comparison, facial skin temperatures were predicted by the physiological model for windy and still air conditions to calculate the WC equivalent temperature. The WC equivalent temperature is defined as the air temperature of an equivalent environment that, under ”calm” wind conditions, entails the same skin surface heat loss to the environment, as in the ”actual”, windy, environment. The simulations were run for various

**Table 2.** Range of boundary conditions considered in the COST 730 validation exercise

| | | Min | max |
|---|---|---|---|
| Air temperature | °C | -17.0 | 50.0 |
| Relative humidity | % | 20.0 | 98.0 |
| air velocity | m/s | 0.1 | 21.9 |
| Solar radiation | W/m$^2$ | 0.0 | 600.0 |
| Metabolic rate | met | 0.8 | 12.1 |
| Clothing insulation | clo | 0.1 | 1.9 |

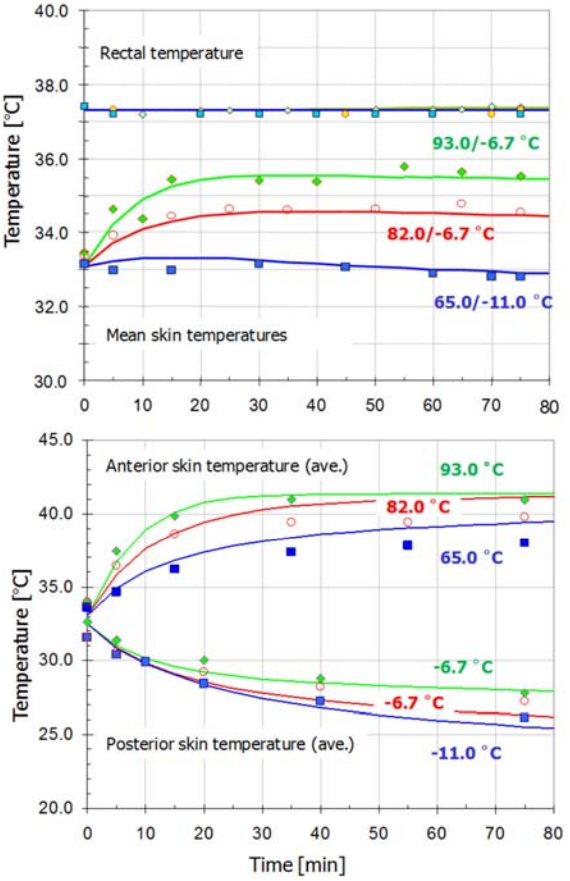


**Figure 15**. Experimental and predicted body core and skin temperature for seminude subjects exposed to extreme radiant asymmetries.

combinations of air temperature and wind speed. As an example, the results obtained for an air temperature of $T_a$= -15 °C and wind speed of $v_a$=40 km/h (10 m above ground) are plotted in Figure 18. The dynamic predictions of the FPC-model approached the final steady-state value in good agreement with WCI (within 1 K). However, the model predicted significantly lower WC-equivalent temperatures for t < 2 hr compared to WCI. These dynamic predictions suggest that during this initial, transient phase (i.e., t<2hr which is most relevant to human exposure to outdoor climate conditions) humans would be much more susceptible to wind-chill than predicted by a steady state model such as WCI.

The inter-model comparisons revealed the best agreement of predicted data for multi-node models. Their two-node counterparts showed greater, partly considerable deviations from the trends of, for instance, mean skin and body core temperatures compared to multi-node models. Figure 19 shows a comparison of the multi-node model of Tanabe *et al* (12) and the FPC-model for a range of outdoor environment conditions. In general, good agreement resulted in particular for the mean skin temperature. Some notable discrepancies between Tanabe and FPC models were observed (not shown in Figure 19) for environmental heat losses and thermoregulatory responses. Suspected reasons included differences in the clothing models used. Generally, good agreement was obtained also between the multi-node Berkeley Comfort Model (13) and the FPC-model, although the deviations in predicted body temperatures were more pronounced.

The COST 730 Validation Exercise - probably the largest and hardest test any physiological simulation model has been subjected to - involved testing the FPC-model against a large number of data from human trial experiments. The work was conducted at different Institutes and involved substantial data analysis in order to validate the model against different climatic conditions, physical exercise and clothing insulation levels. A database of suitable experiments was collected from the literature. Furthermore, the COST Action 730 was in a unique position as several members were able to provide comprehensive, partly unpublished, experimental data from their laboratories. The database contained 58 exposures, each including information on the experimental protocol and the environmental and personal conditions. The range of boundary conditions studied is provided in Table 2 in form of minimum and maximum values. In the experiments 274 test subjects in total were involved.

The experiments also included exposures to outdoor weather situations which were characterized by non-moderate temperatures, elevated and fluctuating air velocities, and solar radiation conditions. The personal conditions covered physical exercise from reclining to hiking with a heavy load, and clothing insulation ranging from bare face exposed to cold wind to protective suits.

An example of an exposure to outdoor climate conditions is shown in Figure 20. In this experiment, the air temperature, solar radiation and metabolic rate while hiking in a hilly area varied during the exposure while the relative humidity (48 ± 4%) and the air velocity stayed at more constant levels. The predictions generally were within one standard deviation from the mean of the experimental data.

A validation example for rather extreme weather conditions with an average air temperature of -13 °C but reaching temporarily a minimum of -18 °C, and an air velocity that fluctuated around 80 km/h on average with a maximum of 178 km/h is provided in Figure 21.

In all investigated cases, the discrepancies between predicted and measured data were quantified using the root-mean-square deviation, *rmsd*, (49). Summarizing all exposures of the COST 730 database, the model reproduced the core temperature with an average *rmsd* of 0.3 ± 0.2 K and mean skin temperature within 1.2 ± 0.7 K.

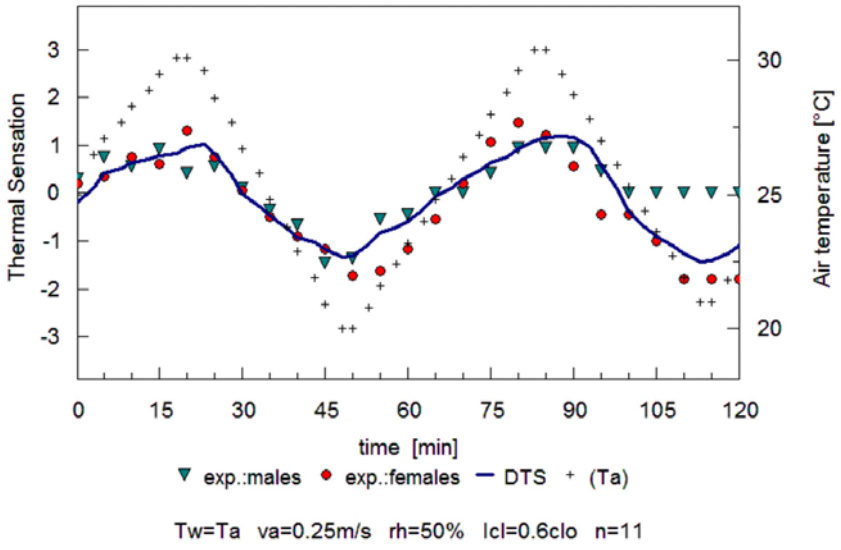


**Figure 16**. Thermal sensation responses to transient environments. periodic changes in air temperature.

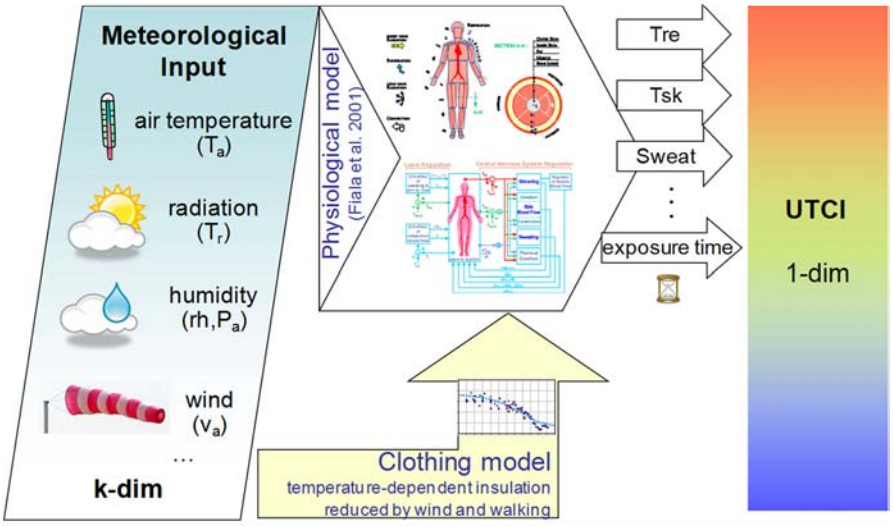


**Figure 17**. Schematic diagram of the procedure constituting the one-dimensional UTC-Index (46).

Both lie within the typical spread of the human physiological response data.

The COST Action 730 work on UTCI has been performed under the umbrella of World Meteorological Organisation's (WMO) Commission on Climatology (CCl). The results will be made available as a WMO *"Guideline on the Thermal Environment"* planned for publication around middle 2010, so that authorities, institutions as well as individuals dealing with biometeorological assessments, in particular National Meteorological and Hydrological Services, universities, public health agencies, epidemiologists, environmental agencies, city authorities, building services engineers, architects and planners can easily apply the new index for their specific purposes.

## 5. THERMOPHYSIOLOGICAL HUMAN SIMULATOR FOR CLOTHING RESEARCH

### 5.1. Introduction

Clothing is the closest envelope of the human body, and hence, has a major impact on the physiological state, thermal comfort and environmental strain of humans. On the other hand, humans and their physiological reactions affect the clothing micro-environment and the clothing properties. For example, the thermal insulation of clothing may be decreased by elevated moisture content from sweating; clothing layers may be heated due to sorption processes. Compression (caused e.g. by wind), pumping effects (e.g. due to body movement), air penetration through fabric, vents and openings also

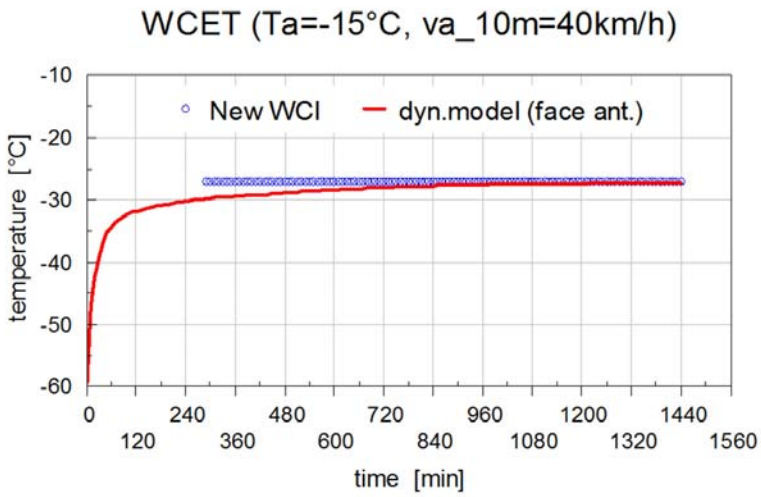


**Figure 18**. Wind Chill Equivalent Temperatures as predicted by the new WC-Index and the dynamic FPC-model.

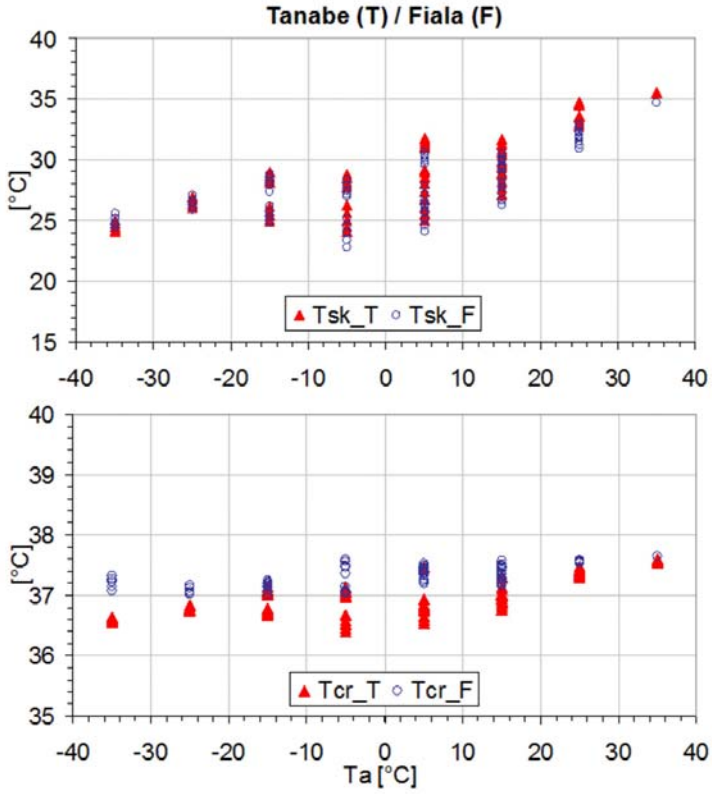


**Figure 19**. Comparison of mean skin temperatures and body core temperatures predicted for a walking person by Tanabe and FPC models for ambient temperature ($T_a$=$T_{MRT}$) ranging between -35 °C and +35 °C (air velocity. 1<$v_a$<18 m/s, relative humidity. RH=50 %, and clothing insulation. 0.4<$I_{cl}$<2.6 clo).

influence dynamically the clothing thermophysical properties.

Current thermal sweating manikins used to study the interactions of the body-clothing-environment are not able to simulate adequately the spatial and transient thermal behavior of humans. Ideally, a human simulator should ”feel” and respond to a given set of environmental conditions as humans do. Various attempts have been undertaken to mimic the human thermal response, for

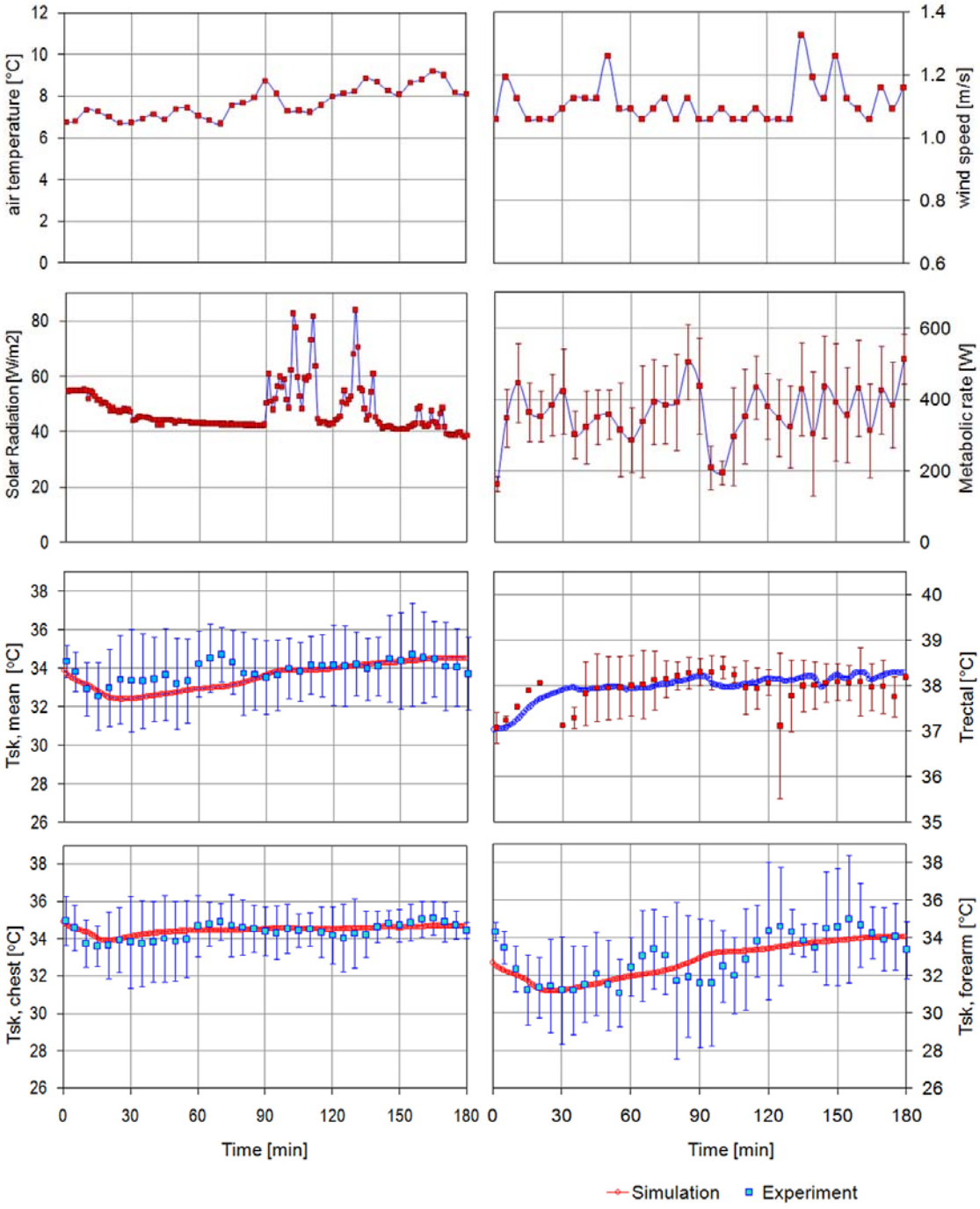


**Figure 20**. Exposure to outdoor weather conditions (48). environmental conditions, local and mean skin temperatures and the rectal temperature as measured (■) and simulated for subjects wearing winter combat suit and long underwear.

instance by adjusting the level of heat input to simulate different workloads, by applying non-uniform surface temperatures over the body, such as cooler hands and feet (50, 51), or applying uniform surface temperatures that change over time (52). Also multi-segmental sweating thermal manikins controlled by a mathematical model of human thermal physiology are being developed to quantify, for example, passenger comfort in vehicles (53). Unfortunately, the discrepancies between body temperatures simulated using manikins and measured in human subjects are still relatively large (54, 55). Nevertheless, all these attempts indicate the growing interest in manikins that adequately simulate human thermal behaviors.

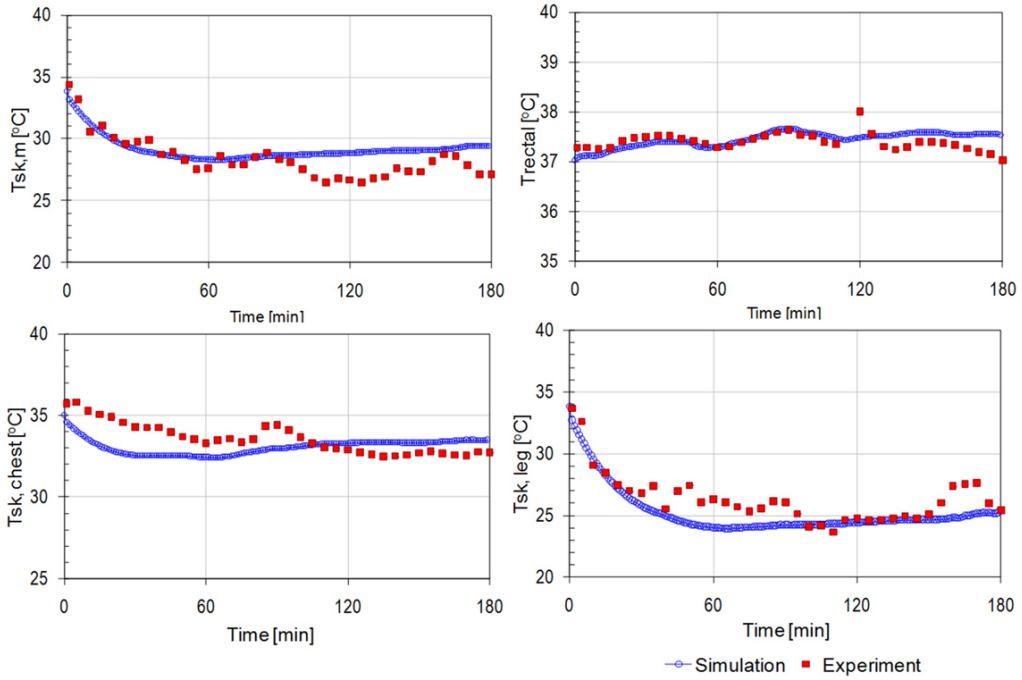


**Figure 21**. Exposure to extreme cold outdoor weather conditions. mean skin, local skin and rectal temperatures as measured (■) and simulated for subjects wearing winter combat suit and long underwear (48).

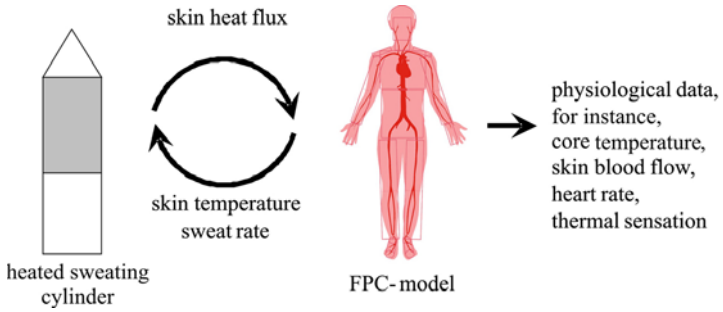


**Figure 22**. Scheme of data exchange in the single-sector thermophysiological human simulator.

### 5.2. Human simulator development

A new single-sector thermophysiological human simulator has recently been developed at Swiss Federal Laboratories for Materials Testing and Research, Empa (29). The motivation for this work was to devise a more accurate measurement instrument that is capable of reproducing the physiological responses of an average human under different boundary conditions. For this purpose a heated sweating cylinder (56) was coupled with the FPC-model.

The single-sector cylinder simulates the entire human body (Figure 22) and the overall human physiological responses. The coupling method is based on real-time exchange of relevant data between the physiological model and the cylinder. The FPC-model provides the area-weighted averages of skin temperature and sweat rate that are used to control the sweating cylinder. The cylinder is sufficiently fast-responding to reach the predicted surface temperature within seconds. The fifty-four sweating outlets and a tight-fitting textile ”skin” enable simulation of uniform sweating. The resultant surface heat loss measured by the cylinder is used as a feedback signal to the FPC-model. This single-value input signal represents the amount of heat exchanged with the actual environment for the actual clothing worn.

### 5.3. Validation study

The human simulator was validated by comparison with results from human subject tests for different environmental conditions. Figure 23 shows three validation examples: for cold, thermo-neutral and hot conditions – each involving semi-nude reclining subjects. The *rmsd* values represent the average differences between the simulations and the corresponding measured data from human experiments (49).

In all the exposures to steady state environmental conditions studied, the thermophysiological human simulator reproduced the body core and skin temperatures

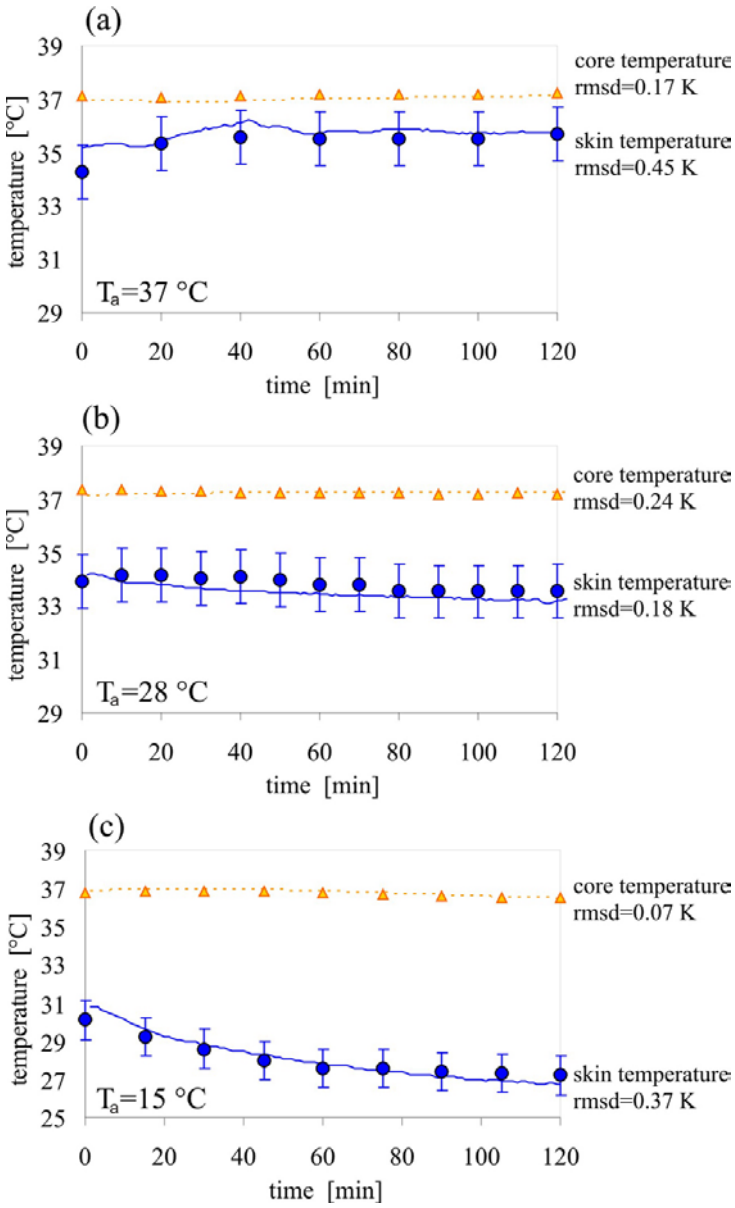


**Figure 23**. Mean skin and body core temperatures of semi-nude reclining subjects as measured (●, ▲) and as predicted (continuous and dashed lines) by the single-sector human simulator for air temperature of (a) 37 °C (57), (b) 28 °C (57), and (c) 15 °C (58).

observed in human subjects with *rmsd* of 0.24 K and 0.62 K, respectively. The validation work also included transient conditions which are of particular interest as the majority of real-life situations are characterized by time-varying environmental and/or personal conditions. For example, the beginning of the cold exposure in Figure 23 (c) represented transients caused by a sudden change in ambient temperature when moving from a pre-test room at ~25 °C to the test chamber at 15 °C. The human simulator reproduced the dynamic physiological response correctly.

The validation tests in Figure 23 were performed for semi-nude subjects, the application range of the human simulator, however, should also include scenarios in which clothing is worn. A comparison of predicted and measured data for two types of "body cover", i.e., a sleeping bag and a nuclear, biological, chemical (NBC) protective suit is shown in Figure 24.

The intended application of the single-sector human simulator is to measure thermophysical properties of a broad range of clothing and sleeping systems under realistic physiological and environmental conditions. This will allow researchers at Empa to design clothing systems that are optimized specifically for protection and comfort of the wearer.

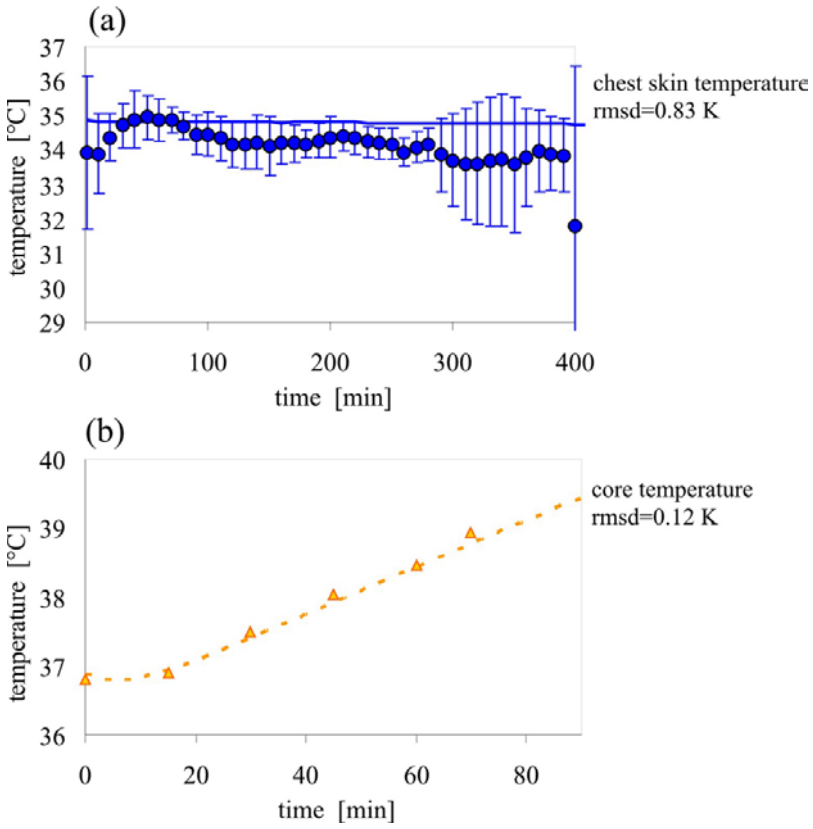


**Figure 24**. Validation examples. (a) Chest skin temperature as measured (●) and predicted (continuous line) for human subjects sleeping in a winter sleeping bag at -18 °C (59), and (b) core temperature as measured (▲) and predicted (dashed line) for human subjects walking in the NBC suit at 35 °C (60).

## 6. THERMAL MANIKIN APPLICATIONS WITHIN AN AUTOMOTIVE SIMULATION SOFTWARE TOOL

### 6.1. Introduction

Virtual development has become an important part of industrial product development processes. Given the financial pressures in today's automotive industry to achieve tough time and quality targets, virtual techniques are essential enabling a large number of load case scenarios and model variants to be analyzed and evaluated in a time- and cost-effective way. Sole experimentation based product development can no longer satisfy the requirements of the automotive industry. Numerical simulation standards, which have their origins in structural mechanics, have thus evolved over time from simple strength analysis to non-linear crash calculations, thermodynamic flow-, indoor climate and occupant comfort simulation and analysis.

State-of-the-art thermal comfort simulation of car occupants involves several disciplines including refrigerant, solar and control technologies, electrical engineering, thermodynamics, heat transfer issues, fluid mechanics, as well human physiology and thermoreception issues. In terms of automotive engineering, this means that the need to model in detail the passenger compartment, the air conditioning and engine cooling systems, the HVAC module, ventilation ducts, and, of course, the car occupants as well as the complex inhomogeneous environmental conditions to which the car occupants are exposed (Figure 25). Thereby, realistic simulation of the moisture and heat transfer processes (conduction, radiation and convection) is required when balancing the heat and enthalpy flows of the entire system – regardless of the numerical scheme used.

Recent advances in mathematical modeling of the human thermal system opened doors for realistic simulation and assessment of occupant comfort under the complex climatic conditions in cars. The algorithms of the FPC-model, as one of the most advanced and widely validated multi-node models, were implemented in the professional thermal simulation software tool THESEUS-FE®. This implicit solver applies the Finite Element Method (FEM) to steady-state and transient heat transfer problems, mainly for use in the automotive industry. The integrated computational manikin, FIALA-FE (21), simulates the human physiology and heat transfer phenomena as originally published by Fiala (14). Both the passive and active systems interact in a fully coupled model that has been shown to agree well with measured human thermal responses over a wide range of environmental conditions.

### 6.2. Thermal manikin integration

Some modifications of the original Fiala theory published in (14) were implemented in order to adopt the computational manikin for purposes of thermal comfort

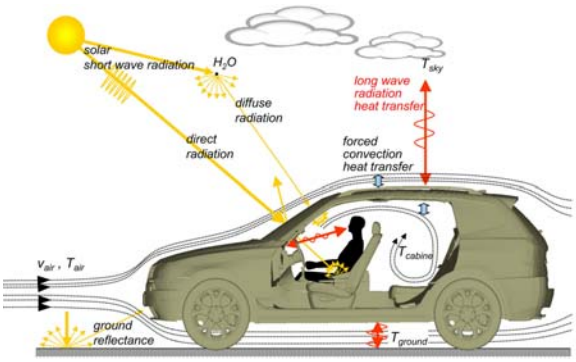


**Figure 25**. Car cabin boundary conditions.

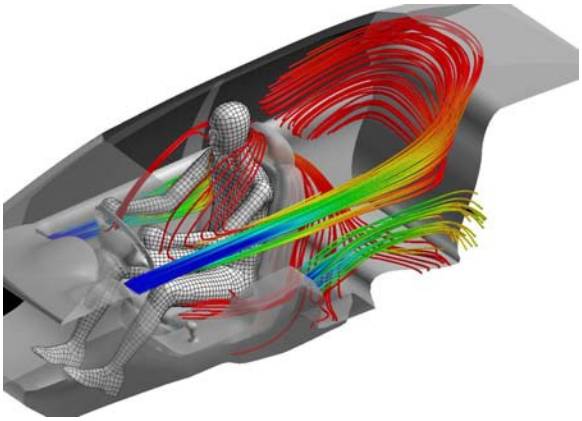

**Figure 26**. Cabin air flow conditions for the case of cooling ventilation.

assessment in cars. The FIALA-FE model consists of 15 body elements. The discretization level for the radial heat conduction is user-adjustable via input of the number of temperature nodes per material layer (e.g. skin, fat, muscle). An additional material layer enables clothing to be simulated individually for each body element sector with user-defined conductive and evaporative resistances, specific heat capacity and thickness. The number of thermal manikins that can be simulated in parallel is unlimited in the simulation system.

Detailed simulation of the convective and radiative heat exchange with the non-uniform enclosure is of particular importance when predicting human thermal and sensation responses in car environments. The incident short wave radiation from the sun transmitted through glazed areas into the car cabin strongly depends on the solar incidence angle. Hot surfaces, frequently the dashboard, transport heat via long wave radiation to cooler surfaces (e.g. exposed human face). Such detailed radiation simulations require calculations of geometry-related radiation factors, i.e., view factors for the exposed surfaces and finite element facets. This information is stored in the so-called *view factor matrix*. In THESEUS-FE, the computationally expensive view factor and ray tracing (to consider shading) calculations need to be performed only once for a given geometry as a pre-processor simulation step. The complexity of the radiation calculations can further be reduced by introducing "patches" (i.e., groups of finite elements with assumed homogenous surface temperatures) which can further notably decrease the preprocessing computation times. Nevertheless, efficient calculation and storage of the *view factor matrix* remains a great challenge even for state-of-the-art software tools.

Realistic simulation of the air flow situation in a car cabin is important when modeling the impact of the convective heat exchange on passenger comfort. In case of ventilation (Figure 26) detailed simulation of local air velocity and temperature patterns is needed to predict the forced convection heat transfer between the occupant body surface and adjacent air. In THESEUS-FE, detailed fluid flow calculations are not part of the simulation process; but results of external CFD simulations can be used as input via appropriate data-transfer interfaces which available as part of the software.

The car's global energy and mass flow balance is constituted by using fully coupled algorithms considering all participating subsystems, the latent heat and mass transfer by respiration and sweating from the human body, the cabin air and the structural parts of the cabin. The conductive heat transfer between the human body and surface elements of the seat are predicted employing algorithms for automated allocation of surface contact zones, Figure 27.

### 6.3. Thermal comfort assessment

Thermal comfort assessment is the ultimate goal of the coupled car cabin – car occupant simulations. Realistic, plausible predictions of the occupants' physiological states including skin and core temperatures are important as these are the input signals into physiological comfort models, such as Fiala's global DTS-index (41) and Zhang's Local Comfort Index (61). These comfort models make then a quantitative assessment of the simulated boundary conditions, design variants and configurations feasible.

Figure 28 shows three variants of heat input in the car seat for a typical winter load case scenario. The initial conditions simulated the driver entering the cold car, being "*very uncomfortable"* due to cold discomfort. Subsequently, the cabin air temperature rose slowly with time due to the injection of warm air by ventilation and the seat heating system started operating and warming up the driver at the contact interface. The conductive heat transport induced a rise in local skin temperature in the contact zones which finally "caused" the driver to become thermally comfortable (*version B* and *C*). Once the cabin air temperature achieved comfortable levels, the additional seat heating is no longer needed and should be switched off automatically. In Figure 28 the *"version B"* variant (green curve) produced the desired maximum local thermal comfort. In contrast, *"version A"* heated up the seat too much which resulted in *"very uncomfortable"* conditions. Here, the Local Comfort Index not only delivered the predicted local perception, but also provided the maximum achievable thermal comfort for each body sector (dashed line).

**Figure 27**. Predicted seat-contact zones.

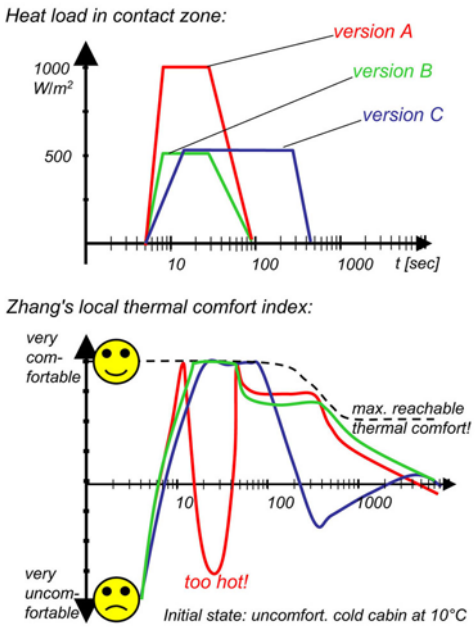


**Figure 28**. Seat heating system comfort assessment.

Recent multi-node mathematical models of human physiology and thermal comfort make plausible comfort assessment of the complex indoor climate conditions in cars possible. Coupled with detailed car thermal management and CFD simulation the FPC-model provides CAE specialists with a powerful method for virtual designing and optimization of modern vehicles specifically for occupant comfort. It can therefore be expected that, in future, this technology will further penetrate and influence the virtual product design and development process in the automotive industry.

## 7. HIGH-RESOLUTION MODELS OF HEAT TRANSFER AND THERMOREGULATION IN HUMANS

### 7.1. Introduction

The development of detailed, high-resolution computational models for bioheat transfer applications represents a significant, enabling technology for clinical hyperthermia applications, and for dosimetry for human exposure to non-ionizing radiation from sources that include imaging systems and mobile communications.

New, very high-field MRI systems can produce magnetic fields of 10 T or more, which is roughly 100 times that of the first-generation systems of the late 1970s (62). The high fields may pose risks of significant tissue heating, especially in the fetus during imaging of a pregnant woman (63). Improved dosimetry tools, including a method to predict tissue temperatures over time and with high spatial resolution, can be invaluable in identifying potential hazards from imaging.

Various hyperthermia protocols have been used for decades to treat tumors, though with mixed, limited success (64). New strategies for thermally-based treatments require delivery of a localized, hyperthermia "dose" to a tumor or neoplasm to target drug delivery. A drug encapsulated in a thermally-labile liposome, for instance, can be administered systemically and released at the tumor site by mild, targeted hyperthermia. This delivery method may enhance drug uptake and tumor regression (65). Clinical application of this technique would presuppose a method for non-invasive, localized heating of a tumor to a target temperature and over a defined time period. These are but a couple of potential applications of high-resolution models of heat transfer and thermoregulation in humans.

### 7.2. High-resolution voxel models

Unlike compartment or "lumped" models, which are numerically realistic but lack anatomical detail, a typical high-resolution model incorporates a dataset of cubic volume elements, or "voxels". The voxel dataset is generated from two-dimensional gray-scale images (CT, MRI, or other digital images). Each pixel of every two-dimensional image is coded according to tissue type – a process known as "tissue segmentation". The series of two-dimensional images is converted to a three-dimensional, tissue-segmented model. Thermal properties (conductivity, metabolic and blood flow rates) can then be assigned according to the voxel's tissue type.

Tissue segmentation may require assigning a numeric code to each of tens (hundreds) of millions of pixels to generate a high-resolution, whole-body model. Lacking automatic or semi-automatic techniques, segmentation can be a very slow and tedious process. The lack of tools for fast and accurate segmentation represents a significant impediment to the wider use of detailed anatomical models for clinical and dosimetric applications (66).

There are a limited number of tissue-segmented, whole-body voxel models which are based on real human anatomy. Whole-body voxel models have been developed based on representative adult male and female Japanese subjects (67) and an adult male Korean (68). A more widely-available set of models was developed by a team in the U.S. at Brooks Air Force Base (now Brooks City-Base). Those models, which include an adult male and female plus a series of laboratory animals (rat, goat, monkey), have voxel dimensions as small as 0.7 mm. The human models

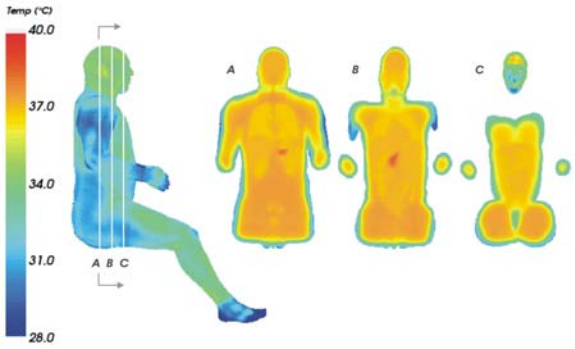


**Figure 29**. Right sagittal surface (a) and coronal section (b-d) temperatures for a man subjected to 45 min. whole-body 100 MHz RF radiation from behind; power density = 4 mW $cm^{-2}$; air temperature $T_a$ = 24 °C.

are based on image sets from the National Library of Medicine's "Visible Human Project®".

Most voxel models were developed for use in dosimetric calculations for exposures to ionizing and non-ionizing radiation. The same voxel models are readily applied to calculation of tissue temperature and thermoregulation effects in humans and animals however, provided the voxel size is sufficiently small. A small voxel size (2 mm or less) is needed to capture anatomical structures or details (such as hypothalamus, skin) which have thermoregulatory significance. As the skin thickness (epidermis and dermis combined) is less than 5 mm over most of the body (69), a relatively coarse model results in surface elements that are a blend of fat and skin tissues (70). This complicates efforts to simulate thermoregulation and surface heat exchange in a realistic fashion.

### 7.3. Radio Frequency Radiation Dosimetry

Human and animal exposure to electromagnetic energy of radio frequency (RF) in the range 100 kHz to 300 GHz can raise tissue temperatures. The heating effect arises from the excitation of molecular dipoles (water molecules) and subsequent energy dissipation within the tissue. In some situations, this energy dissipation can produce profound biological changes. Very high rates of energy dissipation can ablate tissue, for instance. At lower power levels the heating may be more subtle, but the effect yet may be very consequential.

The ability to predict the rate and/or magnitude of temperature increase associated with RF exposure – with a high degree of spatial resolution – can be critical to a variety of clinical applications and provide a rationale for exposure standards to protect human health and safety. Unlike radiation from lasers or ionizing sources, exposure to RF at some frequencies can produce significant internal heating with little increase in the temperature of superficial tissues. For a standing adult man, maximum whole-body absorption, or resonance, occurs at a frequency of approximately 70 MHz (71).

The rate of RF energy absorption in a given tissue volume is known as the "specific absorption rate" (SAR) and is expressed in units of energy, per unit time and per unit mass (W $kg^{-1}$). The local SAR depends on the frequency and power density of the incident electromagnetic field, the body size, shape and orientation, and the electrical properties of the tissue or organ of interest (71). Current exposure standards applicable over most of the RF spectrum generally are based on a presumed maximum safe, whole-body SAR of 0.08 W $kg^{-1}$ for exposure of the general public, and 0.4 W $kg^{-1}$ for "controlled environments" or occupational exposure (72, 73).

The SAR in a tissue volume can be estimated using a finite-difference, time domain (FDTD) algorithm, applied to an appropriate voxel model. The same voxel model can be used for temperature calculations, using the SAR values in the voxel-by-voxel energy balance calculations according to a modified, discretized form of the *Bio-Heat Transfer Equation* (3).

Thermoregulatory response must be incorporated in the model in order to predict realistic body tissue temperatures. The voxel models of the passive system described above were coupled with the FPC cybernetic model of the active system (37). Local values of metabolic and tissue blood perfusion rates and whole-body sweat secretion rates are based on the thermal state of the voxel-ized passive system for each time-step of an exposure simulation.

As an example, Figure 29 illustrates tissue temperatures predicted in a seated adult male exposed from behind to 100 MHz RF for 45 minutes with an average whole-body SAR of approximately 0.27 W $kg^{-1}$. The simulation was performed using a recently-developed code, "ThermoReg" (ThermoAnalytics, Inc., Calumet, MI, USA) applied to the Brooks Man model. The Brooks Man consists of approximately 13 million 2-mm voxels (23). Simulation of a 45-minute exposure required approximately twenty hours of run-time on a four-node, 64-bit system (SGI Altix®, Silicon Graphics Inc., Sunnyvale, CA). For the exposure corresponding to Figure 29, the RF source was posterior to the subject (far-field, EHK orientation). The subject was simulated as semi-nude, wearing cotton shorts only.

The temperatures depicted in Figure 29 suggest surface temperature is slightly elevated from normal pre-exposure conditions. However, internal heating is notable in the abdominal cavity, especially in the pancreas, parts of which reached temperatures approaching 39 °C. Whether this is of any biological or physiological consequence is not yet clear.

The average temperatures of the skin and hypothalamus and the mixed arterial temperatures do not show a substantial change for the same RF exposure as for Figure 29 (100 MHz, 0.27 W $kg^{-1}$ for 45 minutes). Figure 30 shows the temperature histories for an 85-minute simulation at an air temperature of 24 °C, 40 % RH. The exposure protocol consists of (i) 30 minutes thermal equilibration (no RF), followed by (ii) 45 minutes exposure

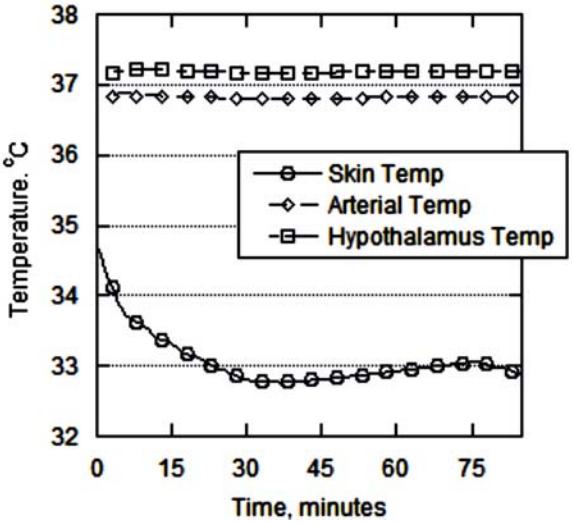


**Figure 30**. Core and skin temperatures during simulated whole-body exposure of seated human to 100 MHz RF.

at 0.27 W $kg^{-1}$ and (iii) 10 minutes of cool-down (no RF). Temperatures were calculated at 30-s intervals. Only every 10th data point is shown in Figure 30, to improve readability.

There is little change in the arterial and hypothalamic temperatures over the course of the simulation. Skin temperature decreases somewhat during the 30-min. equilibration period (no RF), reflecting the relatively cool environment. The weighted skin temperature increases slightly during the ensuing 45-min. exposure and tapers off slightly during the final 10-min cool-off. The skin temperature results depicted in Figure 30 are weighted average values and may not reflect local surface hot spots.

Preliminary results indicate potential usefulness of a high-resolution heterogeneous passive system voxel model which incorporates the FPC active system for simulating the thermal effects of RF exposure. This could present a valuable tool for establishing thermally-based safe exposure standards for radio frequency radiation, and for development of important clinical therapies.

Current efforts are devoted to validating the model and extrapolating results between humans and laboratory animals. Future work will encompass development of improved methods for tissue segmentation, which could enable subject- or patient-specific analysis or treatment planning.

## 8. MODELING INTRA-OPERATIVE TEMPERATURE MANAGEMENT

### 8.1. Introduction

Temperature control by means of active cooling and/or planned re-warming has become an important tool in emergency medicine, intensive care medicine, and peri-operative care practice. Low temperatures are imposed in order to protect organs, especially the brain, during surgery. On the other hand, low body temperatures increase the risk of cardiovascular complications, infections, and shivering. Therefore cooling and re-warming of patients should be tightly controlled in order to reduce or avoid such adverse effects of hypothermia.

Based on the FPC-model, Severens *et al* (74) developed a mathematical model of human thermoregulation under the influence of anesthesia. One of the research foci was to formulate a model that is sufficiently flexible to account for individual patient characteristics and allows local interventions in the open thorax to be simulated. This involved the development of additional numerical sub-models to simulate external heating systems and their role in heating anesthetized patients.

### 8.2. Anesthesia

Anesthesia causes substantial perturbation in the human heat balance. Nearly every patient administered anesthesia becomes hypothermic. The body core temperature can decrease by 1 to 3 °C, depending on the type and amount of anesthesia, the surgery exposure time, the room temperature and the thermal insulation of the body cover (75). In peri-anesthetic patients autonomic thermoregulatory responses, such as peripheral vasomotion, are considerably impaired. In addition, no behavioral temperature regulation takes place which, under normal circumstances, is an effective regulatory response. General anesthesia causes the body temperature thresholds, at which autonomic thermoregulatory reactions are triggered, to shift towards values that significantly deviate from 37 °C.

During cardiac surgery the body is often cooled by means of a heart lung machine. Towards the end of bypass, pump heating is used to induce re-warming the patient. Recent studies have shown that peripheral temperatures respond slower to cooling or heating of the extracorporal blood compared to the body core temperature (75, 76). This effect is involved in the so-called afterdrop in core temperature that may occur after discontinuation of cardiopulmonary bypass. Afterdrop is a rapid decrease in temperature of the re-warmed core caused by ceasing of vasoconstriction and hence increased blood flow into and from the (cooler) periphery (Figure 31). The afterdrop may trigger shivering and increase the risk of post-operative complications.

### 8.3. Forced air heating systems

Covering the inadequately warmed periphery with forced-air heaters during systemic re-warming on bypass reduces post-bypass decrease in core temperature (Figure 31). One intuitional explanation is that cutaneous warming increases peripheral temperature. This would lead to a lower core-periphery gradient, which consequently minimizes the afterdrop. Measurements and analysis of Rajek *et al* (77) did not support this explanation. In fact, it has recently been shown by simultaneous measurements of body temperatures and peripheral blood flow that forced air heaters do not lead to relevant elevation of deep peripheral temperature and skin blood flow (78). The results indicate that the extra heat from forced air heaters is more directly transported from the skin capillaries to the heart and from there redistributed to the core organs.

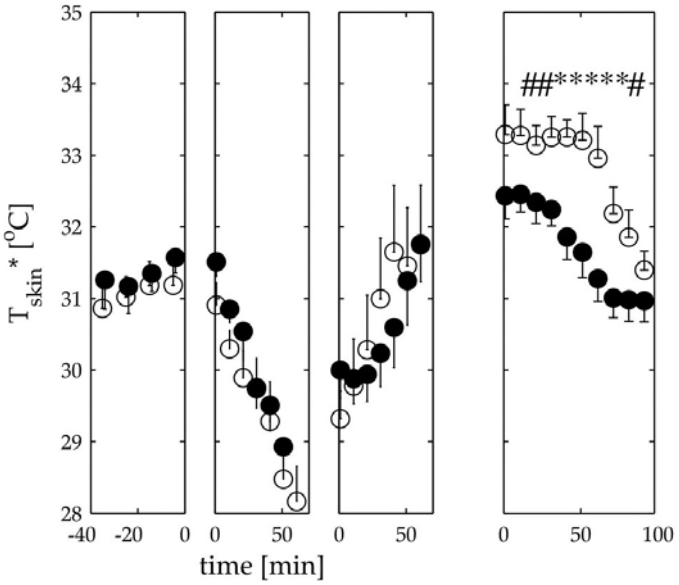


**Figure 31**. Course of the mean skin temperature (average with standard error) measured in patients undergoing, from left to right. anesthesia, cooling, warming and post-bypass; ● control group (without heating blanket), ○ test group. Significant differences ($P<0.05$) are assigned by *, clinical relevant differences ($P<0.10$) by #.

**8.4. Modeling body temperature during cardiac surgery**

The simulation model consists of three parts (Figure 32): (i) the passive system, which is a simplified description of the human geometry and the passive heat transfer processes occurring in the body, (ii) an active part which simulates the thermoregulatory system as a function of the amount of anesthesia and (iii) submodels to adjust and simulate the boundary conditions and individualized body characteristics (25). The passive part of the model is largely based on the original, simplified Fiala *et al* model (27) extended for individual patient characteristics (24).

The active part, i.e., the thermoregulatory system, is restrained to predict vasoconstriction only as non-shivering thermogenesis does not occur during general anesthesia (79) and shivering is prevented by muscle relaxants. The model though takes into account the metabolism-tissue temperature relations (Q10), a decrease in metabolism by 30% due to anesthesia, and blood flow temperature relations for inner skin layers and skeletal muscle tissues. The vasoconstriction model was originally developed using propofol as the main anesthetic agent. The intravenous anesthetic propofol lowers the thresholds for vasoconstriction in linear proportion to increased plasma concentration (79). A linear relationship was derived between the anesthesia concentration and the vasoconstriction threshold. In order to predict propofol concentrations and distribution we used one of the few physiologically based models available (80) and a lumped model describing the transport processes in individual body compartments.

Finally, submodels were formulated to simulate the required boundary conditions and the individualized body characteristics. In the coupled model, the boundary conditions are constituted by modeling heat exchanges: (i) due to conditioning of the blood stream in the heart lung machine, (ii) considering the thermal insulation of the surgical mattress and (iii) accounting for the thermal effect of the forced-air heating.

The model individualization is accomplished by scaling the standard body geometry (27) in such a way that the body composition data, i.e., height, weight, percentage of body fat, and body shape of the model replicates the patients/test persons in the experiments. The model is based on previous research which has shown that predictions for a specific group can be improved by adopting individualized body characteristics (24).

**8.5. Model validation**

In order to validate the model predictions of the core temperature afterdrop, simulations were run for different temperature protocols. These were then compared with data from measurements conducted with and without forced-air heating.

Core and mean skin temperatures during an aortic valve surgery were measured in seven patients with a mean weight of 80.8 kg, height of 172 cm, and fat percentage of 31.8%. They were cooled with the help of a heart lung machine to a nasopharyngeal temperature of 30 °C. Towards the end of the surgery, the patients were re-warmed by the heart lung machine. No forced-air heater was used. The predicted core temperature trends agreed very well with the corresponding measurements (Figure 33). The predictions were not significantly different from the measurements, i.e., were within the range of standard deviations. The modeled and measured skin temperatures initially deviated by up to 2 K because of unknown initial conditions, but eventually the simulation followed the pattern of the measured skin temperature well. That is, the

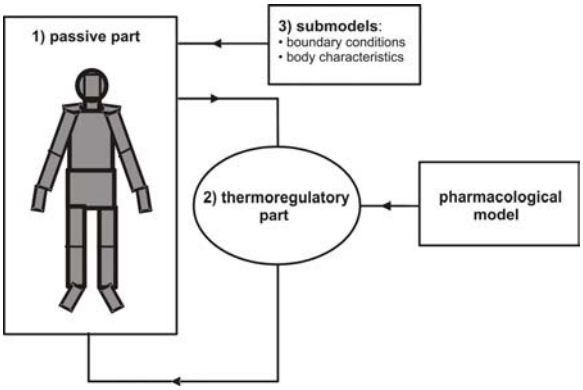


**Figure 32**. The human thermal model. 1) the passive part, 2) the thermoregulatory part coupled with a pharmacological model and 3) submodels accounting for boundary conditions and body characteristics.

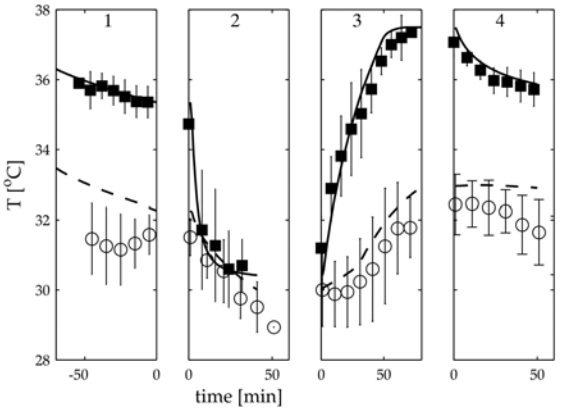


**Figure 33**. Comparison of model simulations with 30% decreased metabolism and measurements without forced-air heating. The surgery consisted of four stages. 1. anesthesia. 2. cooling and 3. re-warming via heart lung machine, and 4. the post-bypass stage; ■ and ○ represent experimentally measured core and mean skin temperatures, respectively, - - and — are the corresponding quantities predicted by the model.

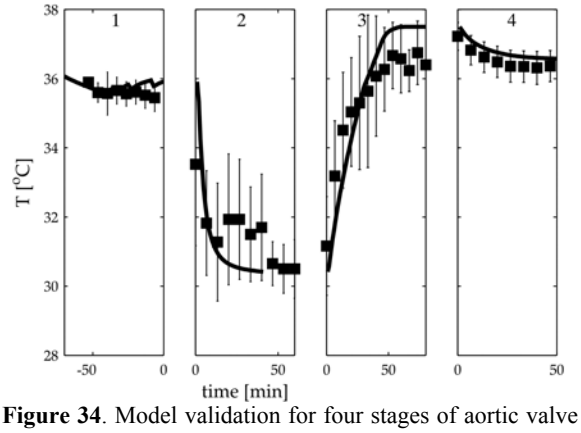


**Figure 34**. Model validation for four stages of aortic valve surgery. 1. anesthesia, 2. body cooling via heart lung machine, and 3. body re-warming by means of both heart lung machine and forced-air blanket, and 4. post-bypass stage involving forced-air blanket.

predictions were not significantly different from the measurements (phase 2, 3, and 4 in Figure 33).

Another validation test was performed for the same type of aortic valve surgery, but with the addition of a forced-air heater in the re-warming and post-bypass stage. The studied group involved 8 patients with a mean weight of 78.6 kg, a height of 169 cm and a fat percentage of 36%. As shown in Figure 34, the predicted core temperature agreed well with measured data also for this case of re-warming (not significantly different from the measurements).

When fully developed, the new coupled simulation model will be used to support and inform clinicians of the effects of possible thermal interventions during cardiac surgery.

## 9. SUMMARY AND CONCLUSIONS

The motivation for the FPC modeling work was to make products of fundamental physiological research available to scientists, engineers, and designers. Various recent applications of the FPC-model underscore the need for physiological modeling tools and for coupled human-environment interaction simulation systems for application in today's interdisciplinary engineering environments. Such tools are essential to the development of optimized ergonomic technological solutions.

This contribution presented the FPC-model and gave an overview of current simulation endeavors, validation studies, and advances in modeling human heat transfer problems in technical and clinical applications. The modeling applications discussed were drawn from diverse fields, including biometeorology, clothing research, thermal comfort assessment in cars, intra-operative temperature management and – in conjunction with a high-resolution model – clinical hyperthermia and radio frequency dosimetry. This work demonstrated both the usefulness of the physiological comfort model and a need for further development.

Extensive validation studies requiring simulation of extreme, transient and complex non-uniform conditions have yielded encouraging results. These and the ability to combine the predictive capabilities of the FPC-model with other simulation tools in coupled analysis systems is proving to be important to industrial and research applications. Challenges for future modeling efforts include simulation of physiological and perceptual responses of acclimatized subjects or special populations, along with optimization of existing numerical and physical simulation systems.

## 10. ACKNOWLEDGEMENTS

The authors express their gratitude to: Deutscher Akademischer Austauschdienst (DAAD) for British-German Academic Research Collaboration for travel funding. EU COST (COST Action 730: "Toward a

universal thermal climate index UTCI for assessing the thermal environment of the human being") for travel funding; Dr. Natascha Severens for her work on the development of open-heart surgery models and measurements; Dipl. Math. Peter Bröde for making available graphical material on the UTCI-procedure (Figure 17); Members of COST Action 730 Work Group 1 (chair: Prof. G. Havenith): 'Thermophysiological modeling' for supporting the model validation work; Prof. Igor Mekjavic for providing measured data from field studies on human exposure to outdoor weather conditions (Figure 20 and Figure 21) and Empa, Sankt Gallen for conducting measurements of thermal properties of clothing used in the validation exercise; Dr. Tong Yang for making available graphical material on coupled CFD-FPC simulation (Figure 3); Mr. Hans Nyberg of ThermoAnalytics, Inc. for generating the results depicted in Figure 29 and Figure 30; Joseph-von-Egle Institut and Knoedler Stiftung for financial support of work on modeling thermal sensation responses; and the UK Engineering and Physical Sciences Research Council (EPSRC) for project funding on detailed radiation modeling (GR/R03495/1).

## 11. REFERENCES

1. A.C. Burton: The application of the theory of heat flow to the study of energy metabolism. *J. Nutrition*, 487-533 (1937)

2. V.J. Aschoff, R. Wever: Kern und Schale im Wärmehaushalt des Menschen. *Naturwissenschaften* 45, 477-485 (1958)

3. H.H. Pennes: Analysis of tissue and arterial blood temperatures in the resting human forearm. *J Appl Physiol* 1, 93-122 (1948)

4. A.P. Gagge: A two-node model of human temperature regulation in fortran. In: Bioastronautics Data Book, J.F. Parker Jr. and V.R. West (eds), Washington DC, *NASA SP-3006*, 247-262 (1971)

5. N.Z. Azer, S. Hsu: The prediction of thermal sensation from a simple model of human physiological regulatory response. *ASHRAE Trans* 83(I), 88-102 (1977)

6. A.P. Gagge, A.P. Fobelets, P.E. Berglund: A standard predictive index of human response to the thermal environment. *ASHRAE Trans* 92, 709-731 (1986)

7. P.O. Fanger: Thermal comfort analysis and applications in environmental engineering. Danish Technical Press, Copenhagen (1970)

8. R.J. de Dear, G.S. Brager: Developing an adaptive model of thermal comfort and preference. *ASHRAE Trans* 104(1A), 145-167 (1998)

9. M.A. Humphreys, M. Hancock: Do people like to feel 'neutral'?: Exploring the variation of the desired thermal sensation on the ASHRAE scale. *Energ Buildings* 39(7), 867-874 (2007)

10. J.A.J. Stolwijk: A mathematical model of physiological temperature regulation in man. NASA contractor report CR-1855, NASA, Washington DC (1971)

11. E.H. Wissler: Mathematical simulation of human thermal behavior using whole body models. In: A. Shitzer, R.C. Eberhart (eds): Heat transfer in medicine and biology – analysis and applications, Plenum New York London, 325–373 (1985)

12. S. Tanabe, K. Kobayashi, J. Nakano, Y. Ozeki , M. Konishi: Evaluation of thermal comfort using combined multi-node thermoregulation (65MN) and radiation models and computational fluid dynamics (CFD). *Energ Buildings* 34(6), 637-646 (2002)

13. C. Huizenga, H. Zhang, E. Arens: A model of human physiology and comfort for assessing complex thermal environments. Build Environ 36(6), 691-699 (2001)

14. D. Fiala - Dynamic Simulation of Human Heat Transfer and Thermal Comfort: PhD Thesis, De Montfort University (1998)

15. D. Fiala, K.J. Lomas: Application of a computer model predicting human thermal responses to the design of sports stadia. Proc. CIBSE National Conference, Harrogate: 492-499 (1999)

16. D. Martinez, D. Fiala, K.J. Lomas, and M.J. Cook: Extended comfort envelopes for office buildings with passive downdraft evaporative cooling. RoomVent 2000, 7th International Conference on Air Distribution in Rooms, Reading, Proc. 1: 53-58 (2000)

17. D. Fiala, A. Bunzl, K.J. Lomas, P.C. Cropper and D. Schlenz: A New Simulation System for Predicting Human Thermal and Perceptual Responses in Vehicles. In: D. Schlenz (ed). PKW-Klimatisierung III: Klimakonzepte, Regelungsstrategien und Entwicklungsmethoden. Haus der Technik Fachbuch Band 27, Expert Verlag Renningen, 147-162 (2004)

18. T. Yang, P.C. Cropper, M.J. Cook, R. Yousaf, and D. Fiala: A new simulation system to predict human-environment thermal interactions in naturally ventilated buildings. Proc. Building Simulation, International Conference, Beijing, 751-756 (2007)

19. K. Kubaha - Asymmetric radiation and human thermal comfort: PhD Thesis, De Montfort University (2005)

20. A. Psikuta - Development of an 'artificial human' for clothing research: PhD Thesis, De Montfort University (2009)

21. S. Paulke: FIALA-FE Theory Manual for THESEUS-FE v2.1 (2007), http://www.theseus-fe.com/

22. RadTherm: Technical Documentation. Thermo Analytics Inc. (2006)

23. D.A. Nelson, S. Charbonnel, A.R. Curran, E.A. Marttila, D. Fiala, P.A. Mason and J.M. Ziriax: A High-Resolution Voxel Model for Predicting Local Tissue Temperatures in Humans Subjected to Warm and Hot Environments. *J Biomech Eng* 131(4), 041003 (2009)

24. W.D. van Marken Lichtenbelt, A.J.H. Frijns, M.J. van Ooijen, D. Fiala, A.M. Kester and A.A. van Steenhoven: Validation of an individualised model of human thermoregulation for predicting responses to cold air. *Int J Biometeorol* 51, 169-179 (2007)

25. N.M.W. Severens, W.D. van Marken Lichtenbelt, A.J.H. Frijns, A.A. van Steenhoven, B.A.J.M. de Mol and D.I. Sessler: A model to predict patient temperature during cardiac surgery. *Phys Med Biol* 52, 5131-5145 (2007)

26. G. Jendritzky: Towards a universal thermal climate index UTCI for assessing the thermal environment of the human being. Memorandum of Understanding for the implementation of a European Concerted Research Action designated as COST 730. 160th CSO Meeting December (2004)

27. D. Fiala, K.J. Lomas and M. Stohrer: A computer model of human thermoregulation for a wide range of environmental conditions: the passive system. *J Appl Physiol* 87, 1957-1972 (1999)

28. S. Weinbaum, L.M. Jiji and D.E. Lemons: Theory and experiment for the effect of vascular microstructure on surface tissue heat transfer - part I: anatomical foundation and model conceptualization. *ASME J Biomech Eng* 106, 321-330 (1984)

29. A. Psikuta, M. Richards and D. Fiala: Single-sector thermophysiological human simulator. *Physiol Meas* 29, 181-192 (2008)

30. P.C. Cropper, T. Yang, M.J. Cook, D. Fiala and R. Yousaf: Simulating the effect of complex indoor environmental conditions on human thermal comfort. Building Simulation '09, 11th Internat. IBPSA Conference, Glasgow, Proc. 1367-1373 (2009)

31. R. Yousaf, D. Fiala and A. Wagner: Numerical simulation of human radiation heat transfer using a mathematical model of human physiology and computational fluid dynamics (CFD). In: High Performance Computing in Science and Engineering `07, Ed. W. Nagel, D. Kröner and M. Resch, Trans. High Performance Computing Center Stuttgart, Springer Berlin Heidelberg, Part 8: 647-666 (2007)

32. A. M. Stoll, L. C. Greene: Relationship between pain and tissue damage due to thermal radiation. *J Appl Physiol* 14, 373-382 (1959)

33. P.O. Fanger, B.M. Ipsen, G. Langkilde, B.W. Olesen, N.K. Christensen, S. Tanabe: Comfort limits for asymmetric thermal radiation. *Energ Buildings* 8, 225-236 (1985)

34. K. Kubaha, D. Fiala, J. Toftum and A.H. Taki: Human projected area factors for detailed direct and diffuse solar radiation analysis. *Intl J Biometeorol* 49(2), 113-129 (2004)

35. K. Kubaha, D. Fiala and K. J. Lomas: Predicting human geometry-related factors for detailed radiation analysis in indoor spaces. Building Simulation '03, 8th International IBPSA Conference, Eindhoven, Proc. (2), 681-688 (2003)

36. S.J. Rees, K.J. Lomas and D. Fiala: Predicting local thermal discomfort adjacent to glazing. *ASHRAE Trans* 114(1), 431-441 (2008)

37. D. Fiala, K.J. Lomas and M. Stohrer: Computer prediction of human thermoregulatory and temperature responses to a wide range of environmental conditions, *Int J Biometeorol* 45(3), 143-159 (2001)

38. A.J. Young, S.R. Muza, M.N. Sawka, R.R. Gonzalez and K.B. Pandolf: Human thermoregulatory responses to cold air are altered by repeated cold water immersion. *J Appl Physiol* 60, 1542-1548 (1986)

39. ANSI/ASHRAE Std. 55-2004: Thermal Environmental Conditions for Human Occupancy. American Society of Heating, Refrigerating and Air-Conditioning Engineers, Atlanta, GA (2004)

40. EN ISO 7730: Ergonomics of the thermal environment – Analytical determination and interpretation of thermal comfort using calculation of the PMV and PPD indices and local thermal comfort criteria. International Organization for Standardization, Geneva (2005)

41. D. Fiala, K.J. Lomas and M. Stohrer: First principles modelling of thermal sensation responses in steady state and transient boundary conditions. *ASHRAE Trans* 109(1), 179-186 (2003)

42. M. Richards and D. Fiala: Modelling fire-fighter responses to exercise and asymmetric IR-radiation using a dynamic multi-mode model of human physiology and results from the Sweating Agile thermal Manikin (SAM). *Eur J Appl Physiol* 92(6), 649-653 (2004)

43. J.F. Hall Jr., F.K. Klemm: Thermal comfort in disparate thermal environments. *J Appl Physiol* 27(5), 601-606 (1969)

44. K.C. Parsons: Human thermal environments: the effects of hot, moderate, and cold environments on human health, comfort and performance. Taylor & Francis, London, New York (2003)

45. G. Jendritzky, A. Maarouf, D. Fiala and H. Staiger: An Update on the Development of a Universal Thermal Climate Index. 15th Conf. Biomet. Aerobiol. and 16th Intl. Congress on Biometeorology, ICB02, Kansas City, AMS, 129-133 (2002)

46. P. Broede, D. Fiala, B. Kampmann, G. Havenith, G. Jendritzky and COST 730 Working Group 1: Der Klimaindex UTCI - Multivariate Analyse der Reaktion eines thermophysiologischen Simulationsmodells. In: Gesellschaft für Arbeitswissenschaft (ed.), Arbeit, Beschäftigungsfähigkeit und Produktivität im 21. Jahrhundert. Dortmund: GfA Press, 705-708 (2009)

47. R. Oszewski and M. Bluestein: The new wind chill equivalent temperature chart. *Bull Am Meteorol Soc,* Oct. 05, 1453-1458 (2005)

48. I.B. Mekjavic, B. Simunic, M.E. Keramidas, N. Kocjan, M. Amon, B. Vrhovec: Field laboratory evaluation of the summer and winter clothing ensembles of the Slovene Armed Forces. Annual Potočnik & Rusjan Memorial Days, 21-23 October 2008, Ig, Ljubljana, Slovenia, 2008.

49. R.J. Barlow: Measuring the spread. In: Statistics: A Guide to the Use of Statistical Methods in the Physical Sciences. Eds: D.J. Sandiford, F. Mandl, A.C. Phillips, Wiley, Chichester (1989)

50. E.A. McCullough, B. Jones and J. Huck: A comprehensive database for estimating clothing insulation. *ASHRAE Trans* 91, 29–47 (1985)

51. E.A. McCullough: The use of thermal manikins to evaluate clothing and environmental factors. Proc. 10th Conf. on Environmental Ergonomics (Fukuoka, Japan), 427–430 (2002)

52. S. Tanabe, E.A. Arens, F.S. Bauman, H. Zang and T.L. Madsen: Evaluating thermal environments by using a thermal manikin with controlled skin surface temperature. *ASHRAE Trans* 100, 39–48 (1994)

53. R. Farrington, J. Rugh, D. Bharathan and R. Burke: Use of a thermal manikin to evaluate human thermoregulatory responses in transient, non-uniform, thermal environments. *SAE Int* 2004-01-2345 (2004)

54. J.P. Rugh and D. Bharathan: Predicting human thermal comfort in automobiles. The Vehicle Thermal Management Systems Conference, Toronto, Canada (2005)

55. J.P. Rugh and J. Lustbader: Application of a sweating manikin controlled by a human physiological model and lessons learned. 6th Int. Thermal Manikin and Modelling Meeting, Hong Kong (2006)

56. T. Zimmerli and M. Weder: Protection and comfort - a sweating Torso for the simultaneous measurement of protective and comfort properties of PPE. Proc. 6th Int. Symp. on Performance of Protective Clothing: Emerging Protection Technologies, ed. J.O. Stull and A.D. Schwope, ASTM STP 1273, West Conshohocken, PA, 271–280 (1997)

57. J.A.J. Stolwijk and J.D. Hardy: Partitional calorimetric studies of responses of man to thermal transients. *J Appl Physiol* 21, 967 (1966)

58. J.A.Wagner and S.M. Horvath: Influences of age and gender on human thermoregulatory responses to cold exposures. *J Appl Physiol* 58, 180–186 (1985)

59. M. Camenzind, M. Weder and C. Ducas: Measurements of sleeping bags at very low temperatures. Part 2 - Human Subject Tests. Empa Report, Empa, St. Gallen, Switzerland (2005)

60. R.R. Gonzalez, T.M. McLellan, W.R. Withey, S.K. Chang and K.B. Pandolf: Heat strain models applicable for protective clothing systems: comparison of core temperature response. *J Appl Physiol* 83, 1017-1032 (1997)

61. H. Zhang: Human Thermal Sensation and Comfort in Transient and Non-Uniform Thermal Environments. PhD thesis, University of California, Berkley (2003)

62. A. Kangarlu, L. Tang and T.S. Ibrahim: Electric field measurements and computational modeling at ultrahigh-field MRI. *Magn Reson Imag* 25(8), 1222-1226 (2007)

63. M. Pediaditis, N. Leitgeb and R. Cech: "RF-EMF exposure of fetus and mother during magnetic resonance imaging. *Phys Med Biol* 53(24), 7187-7195 (2008)

64. M.W. Dewhirst, Z. Vujaskovic, E. Jones and D. Thrall: Re-setting the biologic rationale for thermal therapy. *Int J Hypertherm* 21(8), 779-790 (2005)

65. A.M. Ponce, Z. Vujaskovic, F. Yuan, D. Needham and M.W. Dewhirst: Hyperthermia mediated liposomal drug delivery. *Int J Hypertherm* 22(3), 205-213 (2006).

66. M. Caon: Voxel-based computational models of real human anatomy: a review. *Radiat Environ Biophys* 42(4), 229-235 (2004)

67. T. Nagaoka, S. Watanabe, K. Sakurai, E. Kunieda, S. Watanabe, M. Taki and Y. Yamanaka: Development of realistic high-resolution whole-body voxel models of Japanese adult males and females of average height and weight, and application of models to radio-frequency electromagnetic-field dosimetry. *Phys Med Biol* 49(1), 1-15 (2004)

68. C.H. Kim, S.H. Choi, J. Jeong, H.C. Lee and M. S. Chung: HDRK-Man: a whole-body voxel model based on high-resolution color slice images of a Korean adult male cadaver. *Phys Med Biol* 53(15), 4093-4106 (2008)

69. W.S. Snyder, M.J. Cook, E.S. Nasset, L.R. Karhausen, G.P. Howells and I.H. Tipton: Report of the Task Group on Reference Man. Int. Commission on Radiol. Protection (ICRP), Publ. 23 (1974)

70. P. Bernardi, M. Cavagnaro, S. Pisa and E. Piuzzi: Specific absorption rate and temperature elevation in a subject exposed in the far-field of radio-frequency sources operating in the 10-900-MHz range, *IEEE Trans Biomed Eng* 50, 295-304 (2003)

71. J.A. D'Andrea, J. M. Ziriax, and E. R. Adair: Radio frequency electromagnetic fields: mild hyperthermia and safety standards. *Prog Brain Res* 162, 107-135 (2007)

72. IEEE: IEEE Standard for Safety Levels with Respect to Human Exposure to Radio Frequency Electromagnetic Fields, 3 kHz to 300 GHz: IEEE Standard C95.1, *IEEE Std C95.1* (2005)

73. International Commission on Non-Ionizing Radiation Protection: Guidelines for Limiting Exposure to Time-Varying Electric, Magnetic, and Electromagnetic Fields (up to 300 GHz). *Health Phys* 74(4), 494-522 (1998)

74. N.M.W. Severens: Modelling hypothermia in patients undergoing surgery. *PhD Thesis*, Technical University Eindhoven, p. 170 (2008)

75. D.I. Sessler: Perioperative heat balance. *Anesthesiol* 92, 578-596 (2000)

76. A. Rajek, R. Lenhardt, D.I. Sessler, M. Grabenwoger, J. Kastner, P. Mares, U. Jantsch and E. Gruber: Tissue heat content and distribution during and after cardiopulmonary bypass at 17 degrees C. *Anesth Analg* 88, 1220-1225 (1999)

77. A. Rajek, R. Lenhardt, D.I. Sessler, G. Brunner, M. Haisjackl, J. Kastner and G. Laufer: Efficacy of two methods for reducing postbypass afterdrop. *Anesthesiol* 92, 447-456 (2000)

78. N.M.W. Severens, W.D. van Marken Lichtenbelt, G.M.J. van Leeuwen, A.J.H. Frijns, A.A. van Steenhoven, B.A.J.M. de Mol, H.B. van Wezel and D.J. Veldman: Effect of forced-air heaters on perfusion and temperature distribution during and after open-heart surgery. *Eur J Cardiothorac Surg* 32: 888-895 (2007)

79. D.I. Sessler: Mild perioperative hypothermia. *N Engl J Med* 336, 1730-1737 (1997)

80. R.N. Upton and G.L. Ludbrook: A physiological model of induction of anaesthesia with propofol in sheep. 1. Structure and estimation of variables. *Br J Anaesth* 79, 497-504 (1997)

**Abbreviations.** FPC-model: Fiala human Physiology and thermal Comfort-model; CFD: Computational Fluid Dynamics; $T_a$: air temperature; RH: relative humidity; CSP: computer simulated person; DTS: Dynamic thermal sensation; MRT: mean radiant temperature; RH: relative humidity; rmsd: root mean square deviation, NBC suite: nuclear, biological, chemical suit; HVAC: heating, ventilation and air conditioning; CAE: Computer Aided Engineering; RF: radio frequency; SAR: specific absorption rate; FDTD: finite difference - time domain.

**Key Words:** Thermoregulation, Thermal Comfort, Human Heat Transfer, Numerical Simulation, Body Temperatures, Afterdrop, Radio Frequency Radiation, Review

**Send correspondence to:** Dusan Fiala, ErgonSim – Comfort Energy Efficiency, Holderbuschweg 47, 70563 Stuttgart, Germany, Tel: 49-0-7202 409065, Fax: 49-0-711 50421774, E-mail: dfiala@ergonsim.de

**http://www.bioscience.org/current/vol2S.htm**